GL-TR-90-0170 TGAL-90-06

A COMPARATIVE STUDY OF REGIONAL PHASES FROM UNDERGROUND NUCLEAR EXPLOSIONS AT EAST KAZAKH AND NEVADA TEST SITES

I. N. Gupta
W. W. Chan
R. A. Wagner

Teledyne Geotech Alexandria Laboratory
314 Montgomery Street
Alexandria, VA 22314-1581

SEPTEMBER 1990

SCIENTIFIC REPORT No. 2

GEOPHYSICS LABORATORY
AIR FORCE SYSTEMS COMMAND
UNITED STATES AIR FORCE
HANSCOM AIR FORCE BASE, MASSACHUSETTS 01731-5000

SPONSORED BY
Defense Advanced Research Projects Agency
Nuclear Monitoring Research Office
ARPA ORDER NO 5307

MONITORED BY
Geophysics Laboratory
F19628-88-C-0051

The views and conclusions contained in this document are those of the authors and should not be interpreted as representing the official policies, either expressed or implied, of the Defense Advanced Research Projects Agency or the U.S. Government.

This technical report has been reviewed and is approved for publication.

JAMES F. LEWKOWICZ
Contract Manager
Solid Earth Geophysics Branch
Earth Sciences Division

JAMES F. LEWKOWICZ
Branch Chief
Solid Earth Geophysics Branch
Earth Sciences Division

FOR THE COMMANDER

DONALD H. ECKHARDT, Director
Earth Sciences Division

This report has been reviewed by the ESD Public Affairs Office (PA) and is releasable to the National Technical Information Service (NTIS).

Qualified requestors may obtain additional copies from the Defense Technical Information Center. All others should apply to the National Technical Information Service.

If your address has changed, or if you wish to be removed from the mailing list, or if the addressee is no longer employed by your organization, please notify GL/IMA, Hanscom AFB, MA 01731-5000. This will assist us in maintaining a current mailing list.

Do not return copies of this report unless contractual obligations or notices on a specific document requires that it be returned.

REPORT DOCUMENTATION PAGE

Form Approved
OMB No 0704 0188

1. AGENCY USE ONLY (Leave blank)	2. REPORT DATE	3. REPORT TYPE AND DATES COVERED
	September 1990	Scientific Report No.2 Mar 89-Feb 90

4. TITLE AND SUBTITLE
A Comparative Study of Regional Phases from Underground Nuclear Explosions at East Kazakh and Nevada Test Sites

5. FUNDING NUMBERS
PE 62714E
PR 8A10
TA DA
WU AA
Contract F19628-88-C-0051

6. AUTHOR(S)
I.N. Gupta, W.W. Chan, R.A. Wagner

7. PERFORMING ORGANIZATION NAME(S) AND ADDRESS(ES)
Teledyne Geotech
314 Montgomery Street
Alexandria, VA 22314

8. PERFORMING ORGANIZATION REPORT NUMBER
TGAL-90-06

9. SPONSORING/MONITORING AGENCY NAME(S) AND ADDRESS(ES)
Geophysics Laboratory
Hanscom AFB, MA 01731-5000

Contract Manager: James Lewkowicz /LWH

10. SPONSORING/MONITORING AGENCY REPORT NUMBER
GL-TR-90-0170

11. SUPPLEMENTARY NOTES

12a. DISTRIBUTION/AVAILABILITY STATEMENT
Approved for public release;
Distribution unlimited

12b. DISTRIBUTION CODE

13. ABSTRACT *(Maximum 200 words)*

The spectral characteristics of regional phases from East Kazakh, USSR underground nuclear explosions are studied for their dependence on parameters such as m_b (generally related to shot depth) and spatial location (Shagan versus Degelen). The observed results are compared with those from the Nevada Test Site (NTS), where the near-source conditions are better known. Pn and Lg from 25 Soviet nuclear shots recorded at the Chinese Digital Seismic Network (CDSN) station WMQ are analyzed by obtaining spectral and time-domain measurements on each phase. The average amplitude ratio Pn/Lg is found to be stable with m_b but to vary strongly with frequency. For both Shagan and Yucca Flat explosions of similar yield, the reduction in amplitude with frequency is considerably larger for Lg than for Pn. At higher frequencies (3-7 Hz), the amplitude ratios Pn/Lg for explosions from Shagan, Degelen, Pahute Mesa, and Yucca Flat test sites show significant differences that appear to be due to variations in their source medium velocities. Over the frequency range of about 0.5 to 5.0 Hz, Pn/Lg increases by almost two orders of magnitude for the USSR shots and considerably less for the NTS shots. A possible explanation for the observed Lg spectra varying systematically with shot medium velocity is that Lg from USSR explosions is dominated by S* whereas that from NTS shots includes contributions from both pS and S*.

14. SUBJECT TERMS	15. NUMBER OF PAGES
Regional Phases, Pn, Lg, Shagan, Degelen, S*, WMQ	60
	16. PRICE CODE

17. SECURITY CLASSIFICATION OF REPORT	18. SECURITY CLASSIFICATION OF THIS PAGE	19. SECURITY CLASSIFICATION OF ABSTRACT	20. LIMITATION OF ABSTRACT
Unclassified	Unclassified	Unclassified	SAR

SUMMARY

The spectral characteristics of regional phases from East Kazakh, USSR underground nuclear explosions are studied for their dependence on parameters such as m_b (generally related to shot depth) and spatial location (Shagan versus Degelen). The observed results are compared with those from the Nevada Test Site (NTS), where the near-source conditions are better known. Pn and Lg from 25 Soviet nuclear shots recorded at the Chinese Digital Seismic Network (CDSN) station WMQ are analyzed by obtaining spectral and time-domain measurements on each phase. The average amplitude ratio Pn/Lg is found to be stable with m_b but to vary strongly with frequency. For both Shagan and Yucca Flat explosions of similar yield, the reduction in amplitude with frequency is considerably larger for Lg than for Pn. At higher frequencies (3-7 Hz), the amplitude ratios Pn/Lg for explosions from Shagan, Degelen, Pahute Mesa, and Yucca Flat test sites show significant differences that appear to be due to variations in their source medium velocities. Over the frequency range of about 0.5 to 5.0 Hz, Pn/Lg increases by almost two orders of magnitude for the USSR shots and considerably less for the NTS shots. A possible explanation for the observed Lg spectra varying systematically with shot medium velocity is that Lg from USSR explosions is dominated by S* whereas that from NTS shots includes contributions from both pS and S*.

(THIS PAGE INTENTIONALLY LEFT BLANK)

TABLE OF CONTENTS

(THIS PAGE INTENTIONALLY LEFT BLANK)

INTRODUCTION

The geological environment in which a nuclear explosive is emplaced has significant influence on both amplitudes and spectral shapes of seismic signals. Perhaps the most important single parameter is depth of burial; its effect on the generation of teleseismic and regional phases is important for yield determination as well as for source discrimination. An important parameter influencing $m_b(P)$ for a given yield is proximity to the water table, with shots below it having significantly larger $m_b(P)$ than those above it (Gupta *et al.*, 1989b). Other related parameters are gas porosity, medium velocity, and density. The effect of physical parameters such as shot depth or medium velocity on regional phases other than the direct P is largely unknown. However, it is likely that the near-source parameters control the distribution of total seismic energy into various regional phases and their spectral contents. In this study, we make spectral measurements covering a wide range of frequencies on Pn and Lg from underground nuclear explosions from the East Kazakh test site and interpret the observations on the basis of results derived from Nevada Test Site (NTS) explosions, for which the physical parameters and geological structures are much better known.

At regional distances, Lg is often the largest amplitude arrival from both earthquake and explosion sources. Lg has proven useful for detection, source discrimination, and yield estimation of underground nuclear explosions. It is therefore important to understand the generation and spectral characteristics of Lg. Perhaps the most puzzling aspect of Lg from explosions is their spectra's relative richness in low-frequency content compared to corresponding earthquake Lg spectra, at least for the NTS shots (Murphy and Bennett, 1982). This may be due to the influence of shear waves excited by the free-surface interaction of the spherical P-

wavefront emanating from an explosion, referred to as S* (Gutowski *et al.*, 1984). Finite-difference studies suggest that S* becomes an important phase if source depth, h, is less than the predominant wavelength, λ, of the pulse. This means that for most NTS underground shots (depth less than 1 km), the contribution of S* should be significant for frequencies of 1 Hz or less. S* is generated at take-off angles greater than $\sin^{-1}\beta/\alpha$, where α and β are the P and S wave velocities. Thus S* may contribute directly to Lg (Lilwall, 1988) but not to Pn. It should be noted that the explosions used in Murphy and Bennett's (1982) study were all shallower than 500 m, so the low frequencies 0.5 to 1.0 Hz, corresponding to h/λ less than about 0.2, are within the range in which S* is expected to be strong.

SPECTRAL CHARACTERISTICS OF Pn AND Lg FROM EAST KAZAKH SHOTS

We examined the spectra of regional phases from 25 East Kazakh nuclear explosions in order to understand their dependence on source depth and crustal structure. The data set included 17 shots from Shagan and 8 from Degelen regions recorded on the broadband instrument at the Chinese network station Urumchi (WMQ), located about 950 km southeast of the test site. The explosions are listed in Table 1, which includes data from Ringdal and Marshall (1989) for 14 Shagan River explosions prior to the year 1989. Examples of seismograms are shown in Figure 1. For these USSR shots, depths are not known, but m_b should be a rough measure of relative depths. On these recordings at distances of about 950 km, Pg is not well developed, in agreement with an earlier study of regional phases from Soviet nuclear explosions (Gupta *et al.*, 1980). A possible reason is that in a shield region, Pg energy leaks rapidly into S with each surface reflection (Kennett, 1989).

The first arrival Pn was distinct on all records, and the beginning of Lg was assumed to be at a group velocity of 3.5 km/sec. Spectra of Pn and Lg were obtained by applying a 10% cosine taper to time windows of 12.8 and 51.2 sec for Pn and Lg, respectively. These time windows are indicated on the records in Figure 1. The spectra and the spectral ratio Pn/Lg for the explosion of 27 December 1987 (m_b = 6.0) are shown in Figure 2. The most striking difference between the Pn and Lg spectra is the richness of lower (less than about 1 Hz) and lack of higher frequencies in the Lg spectra. Average Pn/Lg amplitude ratios, with correction for noise and no smoothing, were computed for several frequency ranges. Figure 3 shows a plot of average Pn/Lg ratio (in log units) versus m_b for 14 Shagan River explosions for which precise m_b values are available. Results for frequency ranges of both 3-7 Hz and 0.3-1.0 Hz

TABLE 1

17 SHAGAN AND 8 DEGELEN EXPLOSIONS USED IN STUDY

(a) SHAGAN

No.	Date	Time	Lat(N)	Lon(E)	m_b
1*	12 Mar 1987	01:57:17.2	49.939	78.823	5.31
2*	03 Apr 1987	01:17:08.0	49.928	78.829	6.12
3*	20 Jun 1987	00:53:04.8	49.913	78.735	6.03
4*	02 Aug 1987	00:58:06.8	49.880	78.917	5.83
5*	15 Nov 1987	03:31:06.7	49.871	78.791	5.98
6*	13 Dec 1987	03:21:04.8	49.989	78.844	6.06
7*	27 Dec 1987	03:05:04.7	49.864	78.758	6.00
8*	13 Feb 1988	03:05:05.9	49.954	78.910	5.97
9*	03 Apr 1988	01:33:05.8	49.917	78.945	5.99
10*	04 May 1988	00:57:06.8	49.928	78.769	6.09
11*	14 Jun 1988	02:27:06.4	50.045	79.005	4.80
12*	14 Sep 1988	04:00:00.0	49.870	78.820	6.03
13*	12 Nov 1988	03:30:03.8	50.056	78.991	5.20
14*	17 Dec 1988	04:18:06.8	49.818	78.910	5.80
15	12 Feb 1989	04:15:06.8	49.93	78.74	5.9
16	08 Jul 1989	03:46:57.6	49.87	78.82	5.6
17	02 Sep 1989	04:16:57.2	50.02	79.05	5.0

(b) DEGELEN

No.	Date	Time	Lat(N)	Lon(E)	m_b
1	06 Jun 1987	02:37:07.0	49.86	78.11	5.3
2	17 Jul 1987	01:17:07.0	49.80	78.11	5.8
3	20 Dec 1987	02:55:06.7	49.83	78.00	4.8
4	06 Feb 1988	04:19:07.5	49.80	78.06	4.8
5	22 Apr 1988	09:30:06.9	49.82	78.12	4.9
6	18 Oct 1988	03:40:06.4	49.87	78.08	4.9
7	23 Nov 1988	03:57:06.7	49.82	78.07	5.3
8	17 Feb 1989	04:01:06.9	49.87	78.08	5.0

* data from Ringdal and Marshall (1989)

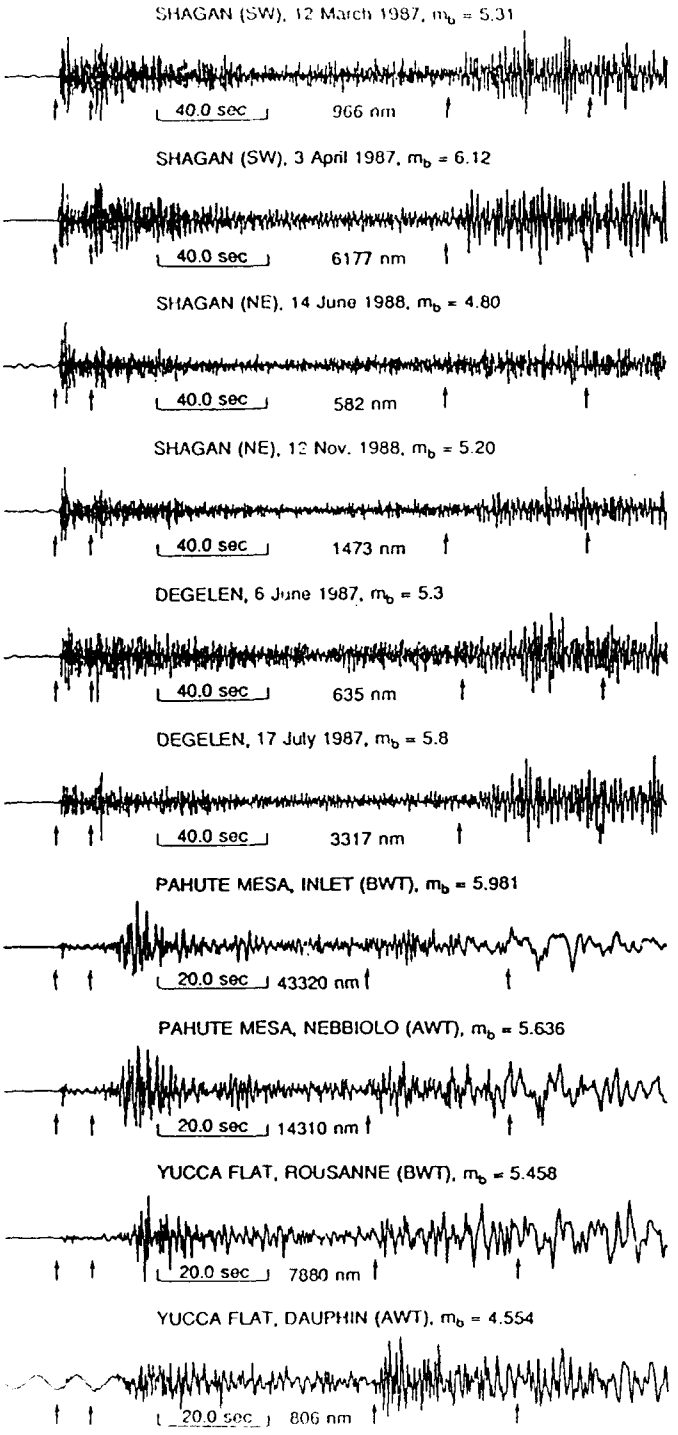

Figure 1. Sample records used in the study. Two records each from southwest Shagan, northeast Shagan, Degelen, Pahute Mesa, and Yucca Flat regions are shown. For the NTS shots, both below and above the water table shots (denoted by BWT and AWT, respectively) are included. The arrows indicate the Pn and Lg windows (12.8 and 51.2 sec for the USSR and 6.4 and 25.6 sec for the NTS shots) used in the spectral analyses.

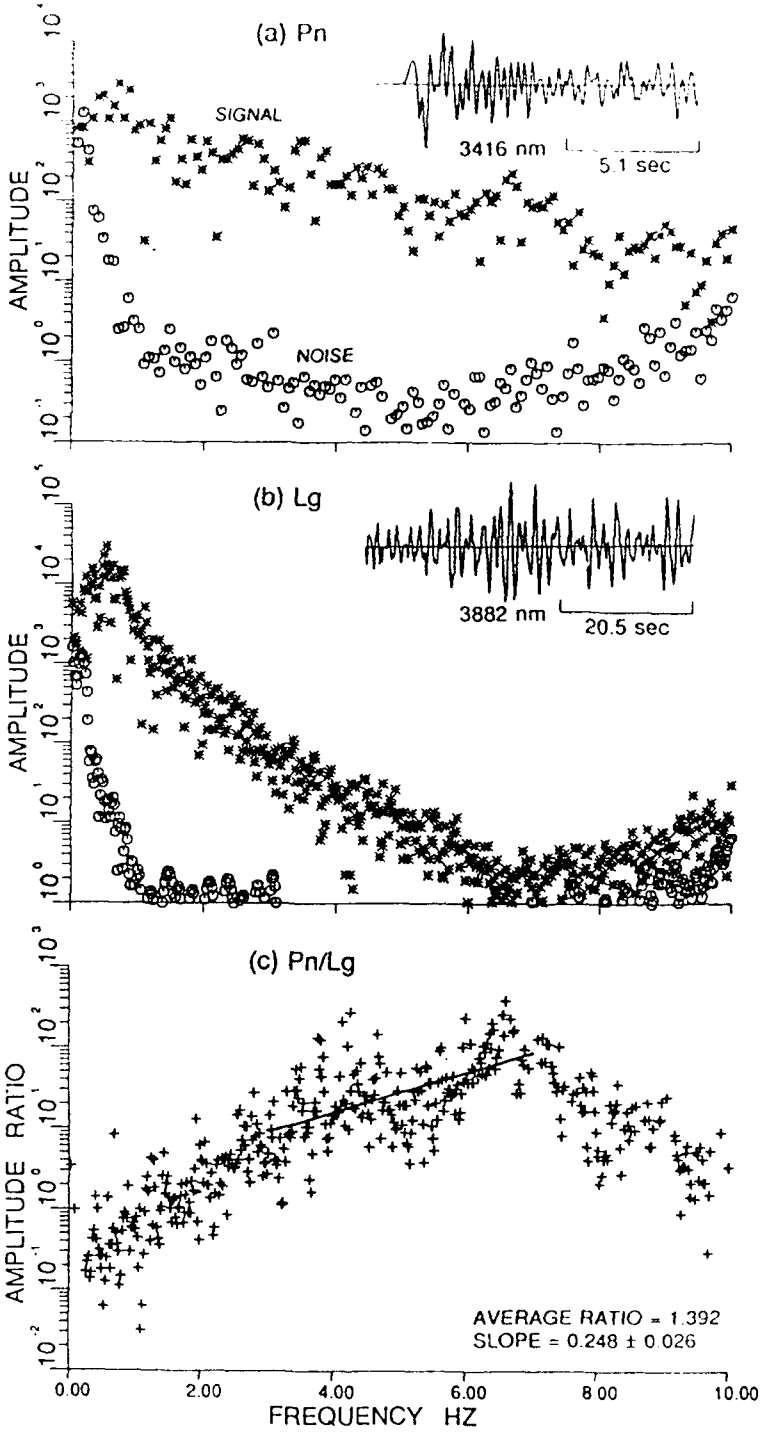

Figure 2. Waveforms and displacement spectra of signal and noise, corrected for instrumental response, for (a) Pn and (b) Lg for the Shagan explosion of 27 December 1987; (c) Spectral ratio Pn/Lg, corrected for noise, points for which S/N power ratio is less than 2 are not plotted. The mean slope and average ratio (in log units), over the frequency range of 3-7 Hz, are indicated.

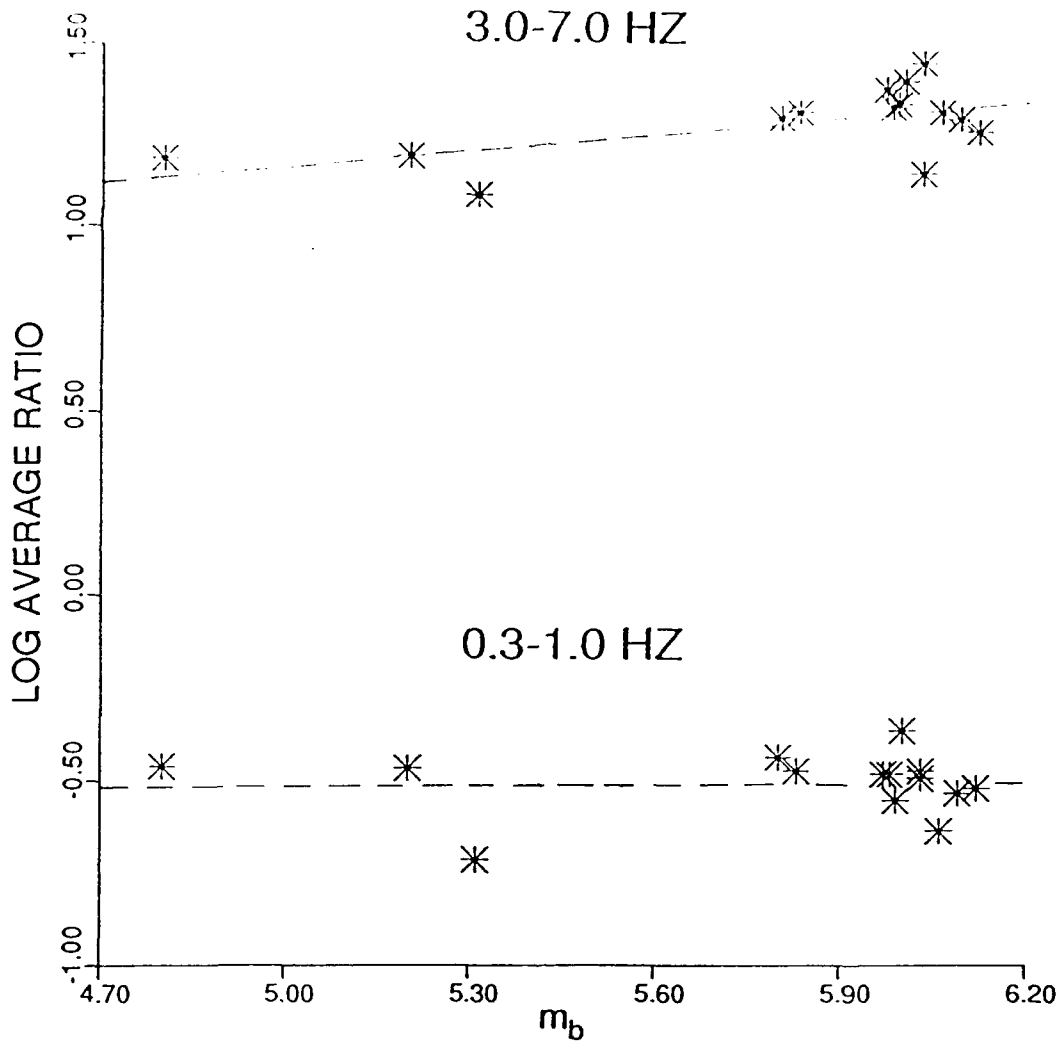

Figure 3. Average Pn/Lg ratio (log units) versus m_b for 14 Shagan explosions for frequency ranges of 3-7 Hz (top) and 0.3-1.0 Hz (bottom). Note the weak dependence on m_b and strong variation with frequency.

indicate no significant variation with m_b, although there is strong dependence on frequency since the two populations are separated by almost 2 log units. For Shagan River explosions, m_b is a fairly good measure of shot depth. Therefore Pn/Lg, measured over a narrow frequency range, seems to be nearly independent of shot depth. In Figure 4, average Pn/Lg values, in log units, over the frequency ranges of 0.3-1.0 Hz and 3-7 Hz are plotted at their epicentral locations. For the higher frequency range (Figure 4a), the Shagan and Degelen events are well separated, with the Degelen shots showing relatively more Lg than Pn. Moreover, the northeast and southwest Shagan explosions also appear to be separated, although there are only three data points for the northeast region. This difference suggests relatively more Lg than Pn in the northeast Shagan region and agrees with Ringdal and Fyen's (1988) teleseismic observations on differences between m_b(P) and m_b(Lg).

We also computed RMS values, corrected for instrument response and noise, for both Pn and Lg phases over several frequency passbands. This was accomplished by removing the mean and linear trend from the observed record, applying taper to the selected regional phase window, obtaining its Fourier transform, applying the instrument response correction, and filtering over the desired frequency band by using a three-pole phaseless Butterworth filter. This was followed by transforming back to the time domain, computing the mean squared values separately for signal and noise windows, correcting for noise by subtracting the mean squared noise from that in signal, and taking its square root. For 14 Shagan explosions with precise m_b available from Ringdal and Marshall (1989), the RMS values for various frequency bands were plotted against m_b for both Pn and Lg. Results for 0.5-1.0 Hz and 4.0-6.0 Hz passbands are shown in Figure 5. For a fixed frequency, the mean slopes for Pn and Lg are nearly the same, but the higher frequency slopes are much smaller than the lower frequency

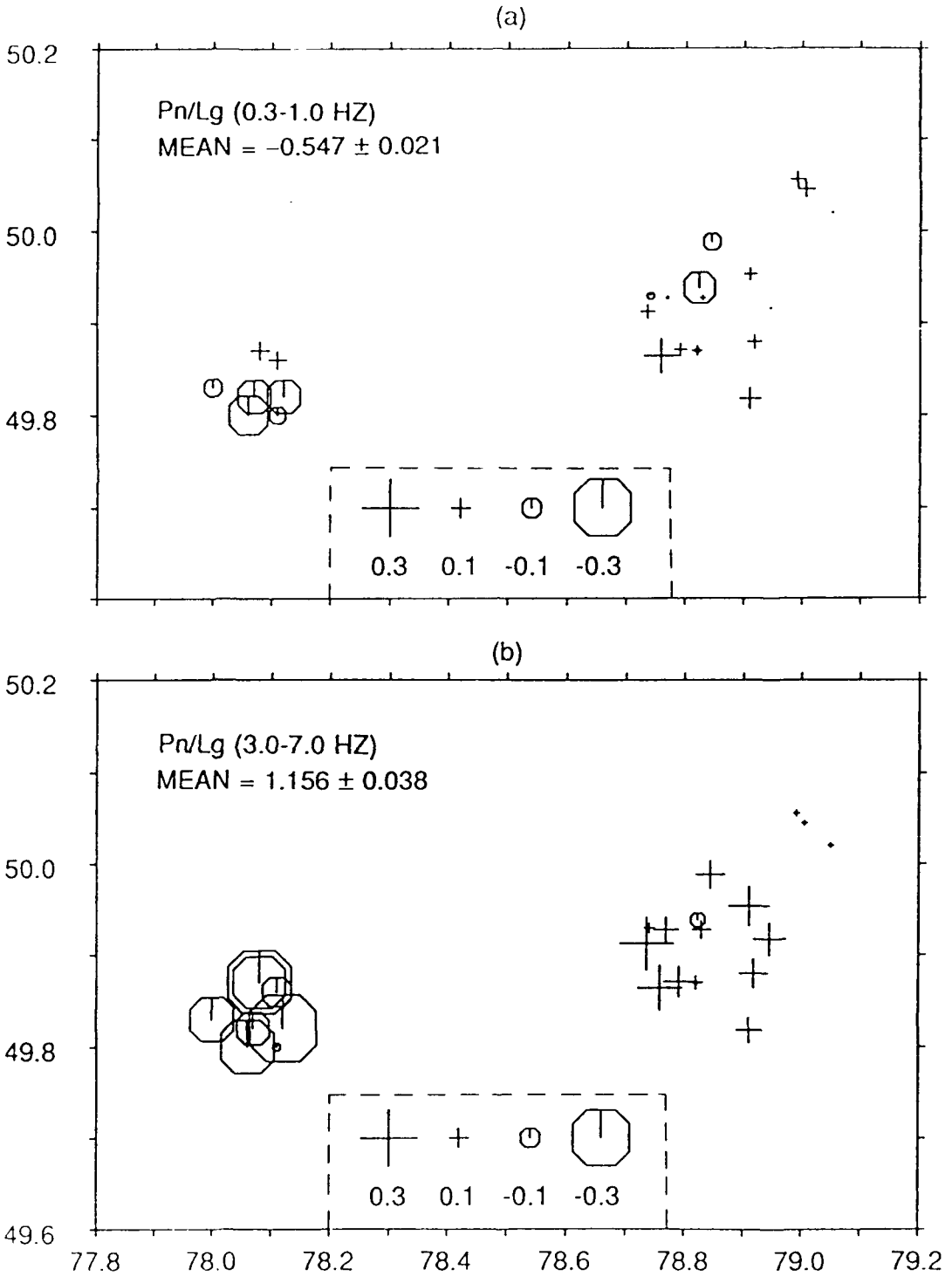

Figure 4. Average Pn/Lg amplitude ratio (in log units and demeaned) for 25 USSR (17 Shagan and 8 Degelen) shots plotted at their geographical locations for the frequency range of (a) 0.3-1.0 Hz and (b) 3-7 Hz. At higher frequencies, the Degelen, northeast Shagan, and southwest Shagan events appear well separated, suggesting differences in local structure.

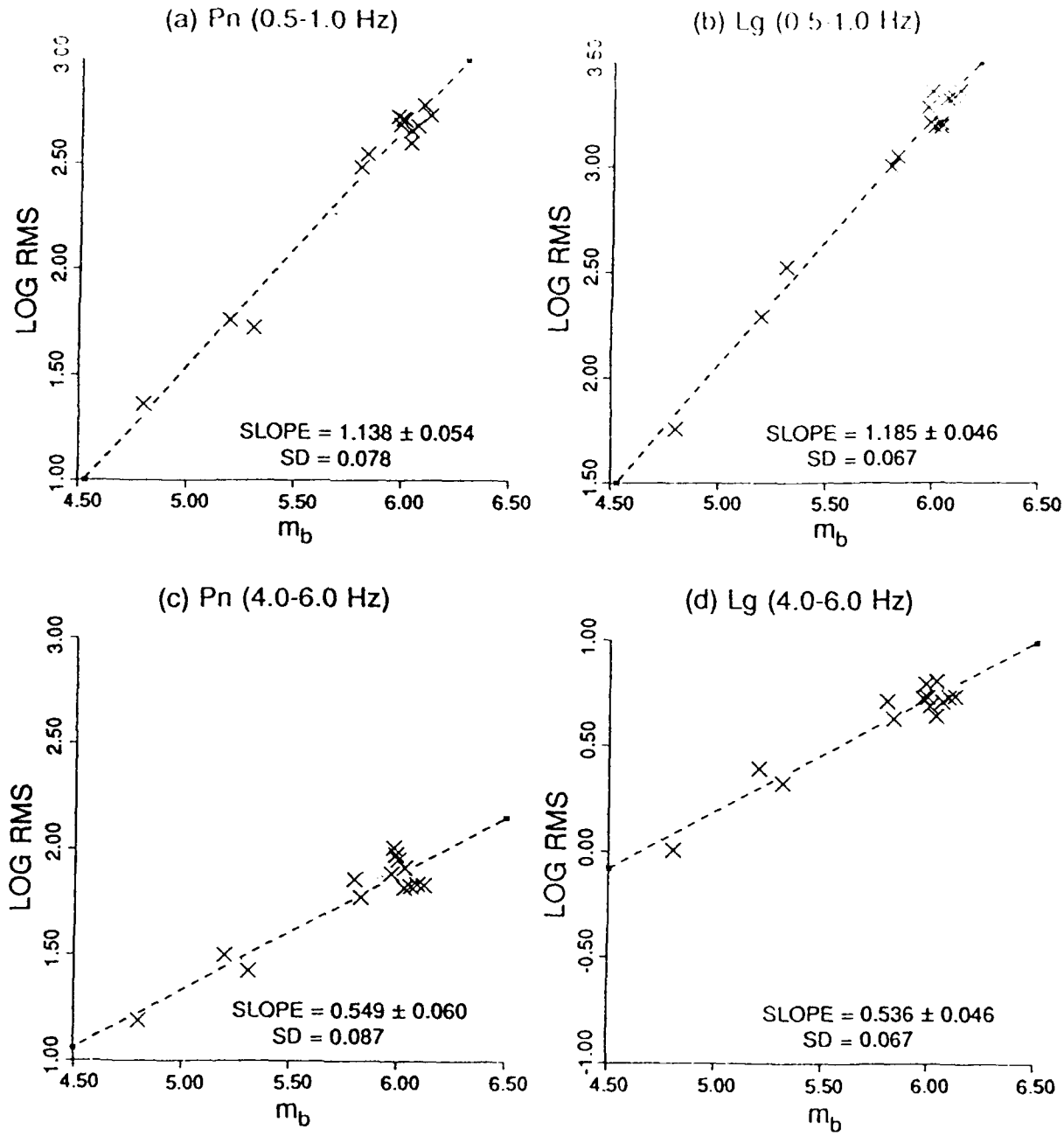

Figure 5. RMS amplitudes of Pn and Lg versus m_b for 14 Shagan explosions for two frequency passbands, as indicated. Each plot indicates the least squares linear regression (dashed line), mean slope (with associated standard deviation), and one standard deviation of residuals (SD). For a fixed m_b, the reduction in RMS at the higher frequency is much larger for Lg than for Pn.

slopes. This dependence of slope on frequency is expected on the basis of source scaling. The slope values are, however, poorly constrained since the data points are not well distributed with respect to m_b. Plots of RMS versus m_b, such as those in Figure 5, were used to compute mean log RMS for Pn and Lg for m_b = 6.0. Results for various center frequencies, shown in Figure 6, indicate Pn and Lg to have vastly different variation with frequency; Pn(RMS) varies by less than 1 magnitude unit (m.u.) whereas Lg(RMS) varies by the significantly larger amount of about 2.5 m.u. The decrease in amplitude with increasing frequency is therefore much faster for Lg than for Pn.

Using all 17 Shagan shots (Table 1), and for frequency bands with the center frequency ranging from about 0.5 to 5.0 Hz, log RMS amplitude ratios Pn/Lg were plotted versus m_b, linear regression fits obtained, and the mean value for m_b = 6.0 computed. The resulting log RMS (Pn/Lg) values are plotted versus center frequency in Figure 7. Similar results derived from 8 Degelen shots are also included in Figure 7. For both Shagan and Degelen explosions, Pn/Lg increases strongly with frequency (by almost two orders of magnitude) and, as suggested by Figure 6, most of the increase is due to Lg diminishing rapidly with frequency. Furthermore, the Pn/Lg values for Degelen shots are about 0.1-0.2 m.u. smaller than those for Shagan explosions for nearly all center frequency values.

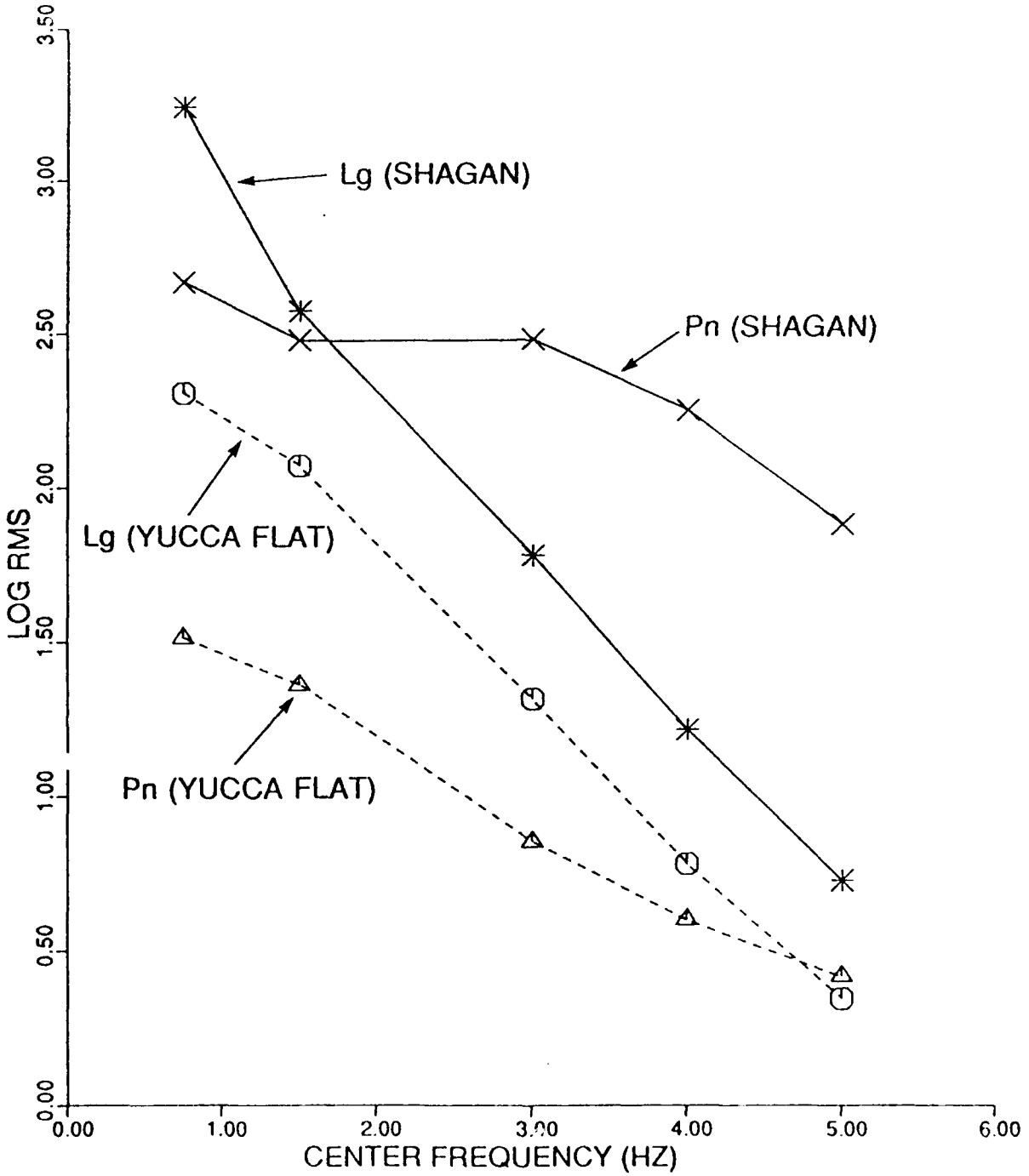

Figure 6. Log RMS versus center frequency of passbands for Pn and Lg for a Shagan explosion of m_b = 6.0 (yield about 110 kt) derived from 14 Shagan explosions. Similar results for a Yucca Flat explosion of m_b = 5.5 (yield about 110 kt), derived from 23 Yucca Flat explosions, are also shown.

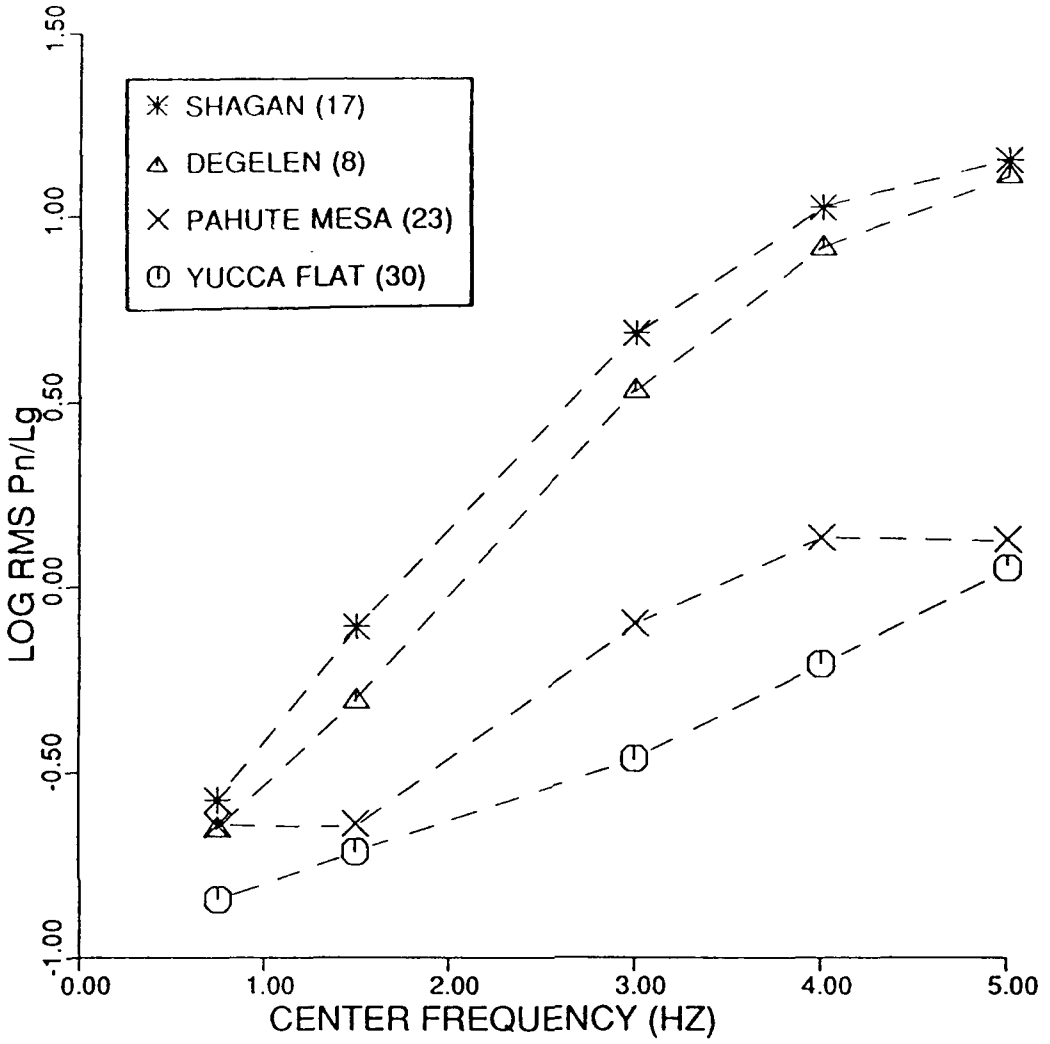

Figure 7. RMS amplitude ratios Pn/Lg versus center frequency of passbands for Shagan and Degelen explosions of $m_b \approx 6.0$. Similar results for Pahute Mesa and Yucca Flat shots of $m_b \approx 5.5$ are also shown. Note the significantly larger increase with frequency for the Soviet shots.

REGIONAL PHASES FROM EXPLOSIONS AT THE NEVADA TEST SITE

Larger bandwidth data often show significant differences in the spectral content of the various regional phases recorded at a common station. As an example, the bandpassed data from the vertical component records of MAST (shot depth = 911 m, m_b = 5.9) and STILTON (depth = 732 m, m_b = 5.8) at the Lawrence Livermore National Laboratory's station ELK are shown in Figure 8. Although both of these shots are from the Pahute Mesa region, their work point velocities (4.2 km/sec and 2.6 km/sec, respectively) are significantly different. The signals are passed through bandpass filters and the envelope shape of the seismogram is defined by rectifying and smoothing the trace. The top trace is the original seismogram, rectified and smoothed, while the bottom five traces are obtained by bandpass filtering into the frequency bands noted on the left, prior to being rectified and smoothed. Whereas Pg appears strong in nearly all frequency bands, Lg is rich in low frequencies only, and Pn is richer in higher frequencies. Furthermore, the coda of Pg appears to trail into Lg for the first two frequency bands. In the original seismograms, Pn/Lg for the lower velocity shot, STILTON, is smaller than that for the higher velocity shot, MAST. A comparison of low- and high-frequency amplitudes suggests the decrease of Lg with frequency at a rate faster for MAST than for STILTON. It seems therefore that differences in the excitation of various regional phases among various frequency passbands may be diagnostic of the near-source environment of an explosion.

Gupta *et al.* (1989a) studied the dependence of P and Lg magnitude-yield relationships on physical parameters such as gas porosity, shot depth, and shot medium velocity. Figures 9 and 10 are based on their results for 102 NTS tuff-rhyolite shots for which overburden (aver-

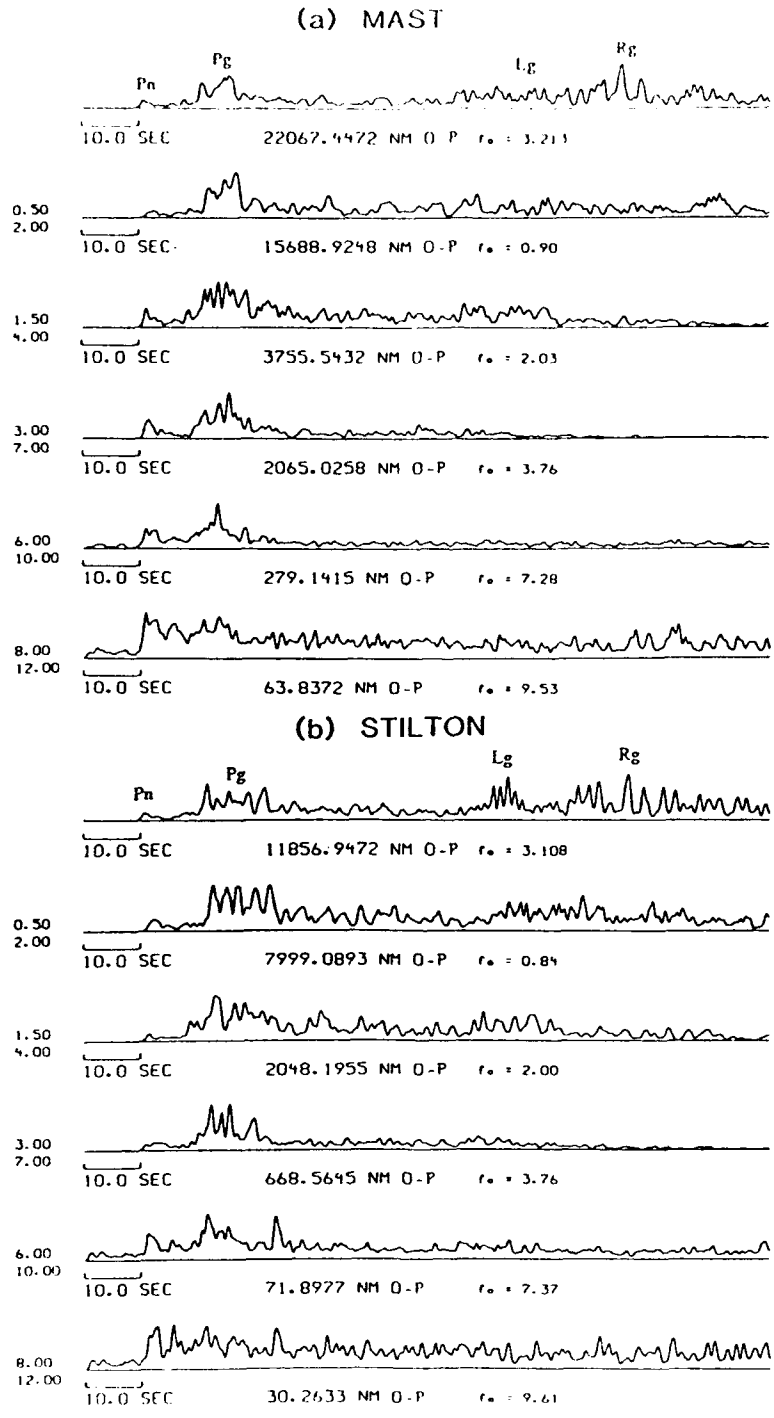

Figure 8. Envelope seismograms from vertical component records of MAST and STILTON at ELK. The traces have been rectified and smoothed and the bottom five traces have been bandpass filtered into different frequency bands. The maximum amplitude and the average frequency (from a count of zero-crossings prior to rectification) are indicated below each trace. Note the frequency-dependent differences in the excitation of various regional phases for the two shots.

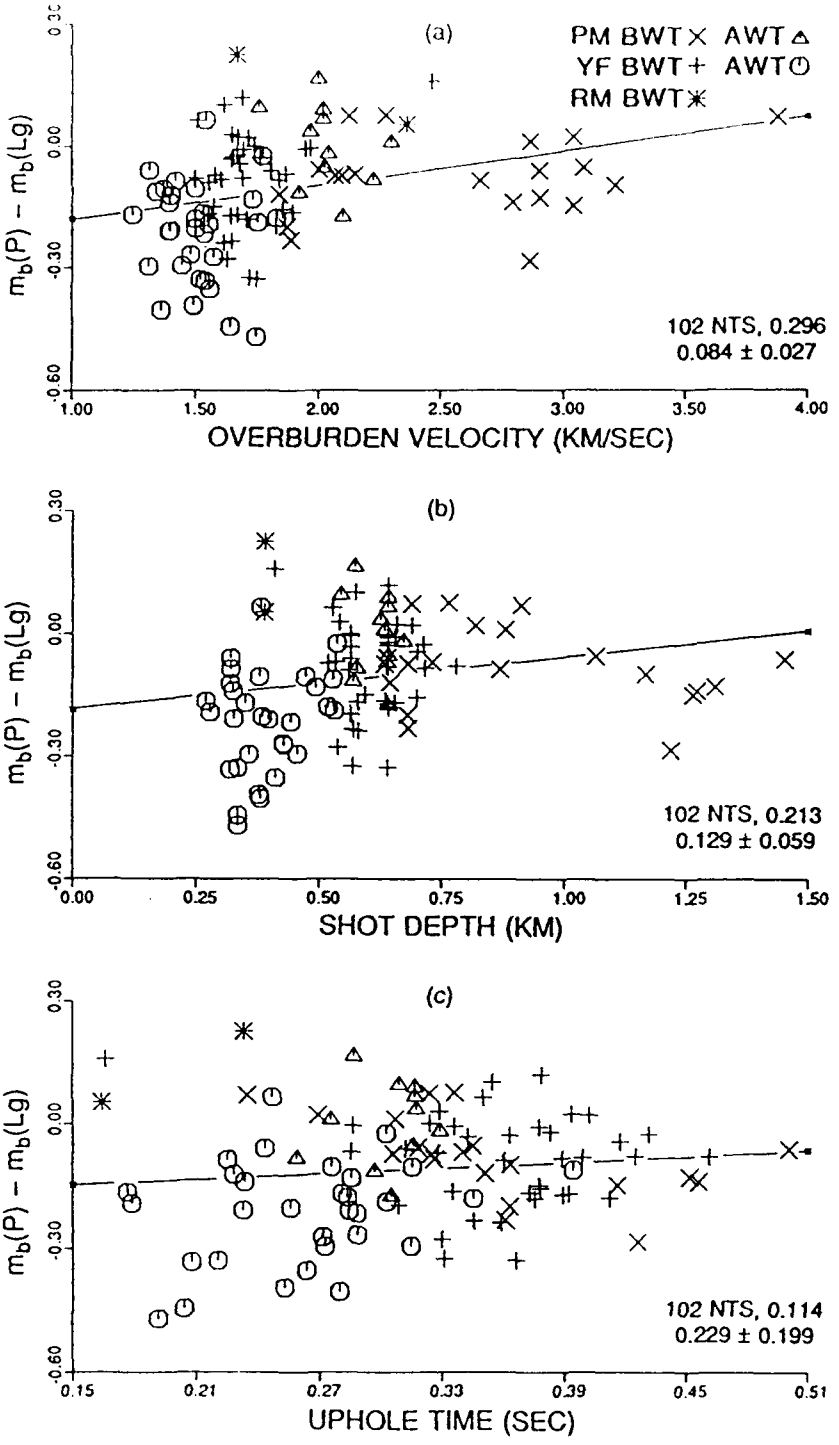

Figure 9. $m_b(P)$ - $m_b(Lg)$ versus (a) overburden velocity, (b) shot depth, and (c) uphole time for 102 NTS tuff-rhyolite shots. Linear regression results are shown and the correlation coefficient and mean slope (with associated standard deviation) values are indicated. The dependence on overburden velocity appears to be relatively stronger than on shot depth and uphole time.

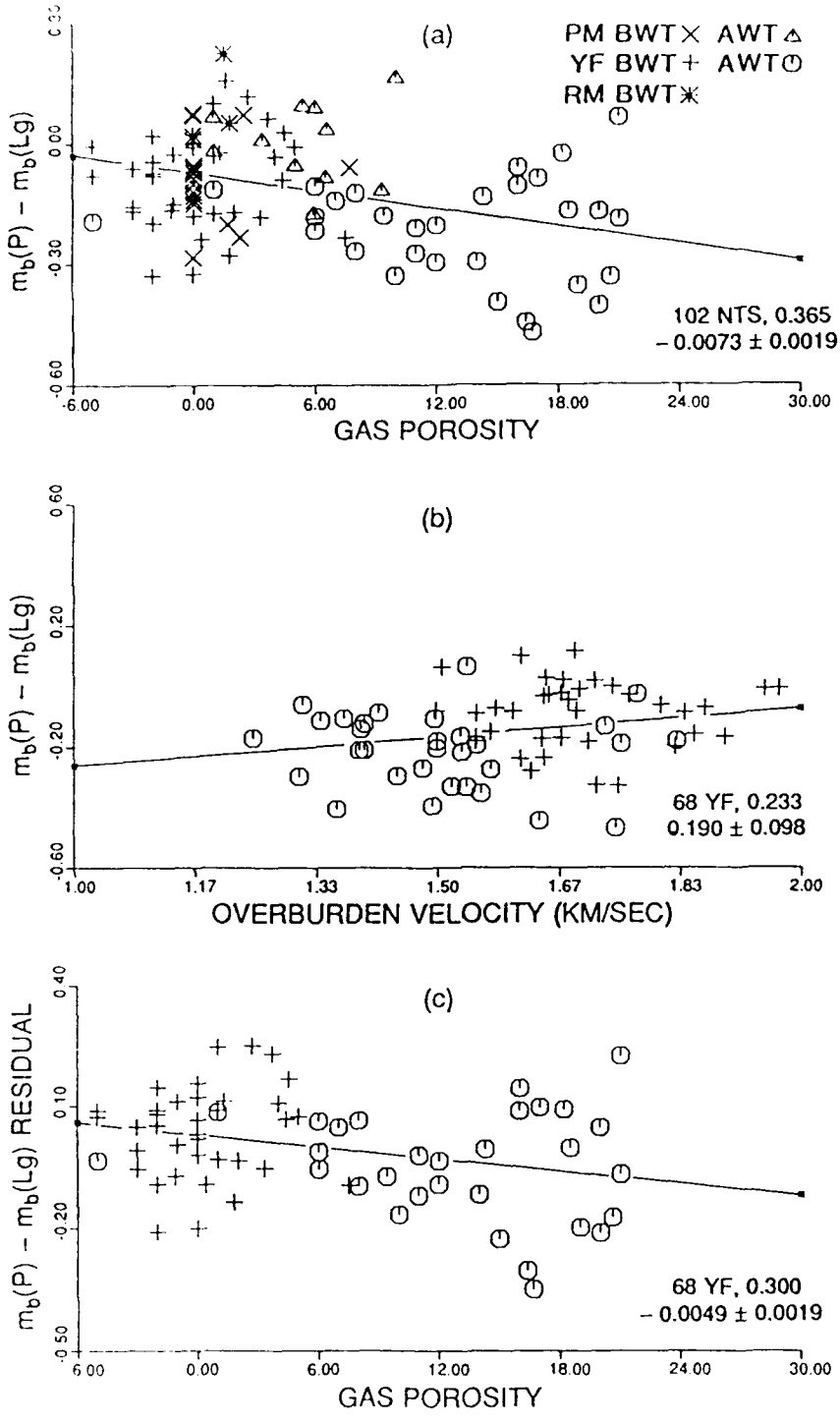

Figure 10. Similar to Figure 9 for (a) $m_b(P)$ - $m_b(Lg)$ versus gas porosity, (b) $m_b(P)$ - $m_b(Lg)$ versus overburden velocity for 68 Yucca Flat explosions, and (c) $m_b(P)$ - $m_b(Lg)$ residual versus gas porosity. Dependence on gas porosity is not significant when the data are corrected for the effect of overburden velocity.

age of work point to surface) velocity, gas porosity, m_b(P) (P. D. Marshall, written communication), and m_b(Lg) (Patton, 1987) were available. The data set consisted of 69 Yucca Flat (YF), 39 Pahute Mesa (PM), and 2 Rainier Mesa (RM) shots and included both below the water table (BWT) and above the water table (AWT) shots. The regression in Figure 9a suggests some dependence on overburden velocity, consistent with relatively larger Lg for lower velocity media. The dependence on shot depth (Figure 9b) is somewhat weaker than on overburden velocity. From theoretical considerations, the uphole time (shot depth)/(overburden velocity) is more likely to be the parameter controlling the generation of seismic waves than the shot depth, but the regression in Figure 9c indicates poor dependence. Therefore, it seems that the relative excitation of P and Lg is influenced by medium velocity and not by shot depth; the apparent dependence with shot depth is perhaps due to the fact that overburden velocity and shot depth are correlated since the medium velocity generally increases with depth.

Figure 10a shows a plot of m_b(P) - m_b(Lg) versus gas porosity, and it may seem that there is significant dependence. However, this may be due to the fact that gas porosity correlates well with overburden velocity. In order to test this, data from Yucca Flat shots with large variations in both overburden velocity and gas porosity were selected. Pahute Mesa shots were excluded because a large number of them had porosity equal or close to zero. A plot of m_b(P) - m_b(Lg) for 68 Yucca Flat shots versus overburden velocity (Figure 10b) was used to obtain the corresponding residuals which were then plotted versus gas porosity (Figure 10c). The weak dependence between the two parameters in Figure 10c suggests that the difference between P and Lg amplitudes is insensitive to gas porosity when the data are corrected for the effect of overburden velocity.

We analyzed the spectral characteristics of Pn and Lg phases from 53 NTS (30 Yucca Flat and 23 Pahute Mesa) shots well recorded at ELK; a few examples are shown in Figure 1. Most of these shots were in tuff and rhyolite, but 6 Yucca Flat shots were in alluvium. Since the source-receiver distances for these shots are only about 400 km, the time windows for Pn and Lg were taken to be 6.4 sec and 25.6 sec, respectively. As an example, the spectra and the spectral ratio Pn/Lg from the Yucca Flat explosion ROUSANNE ($m_b \simeq 5.5$) are shown in Figure 11. Comparison with a Shagan explosion of similar yield (Figure 2) shows significant differences between both spectra and spectral ratios. For Pn, the reduction in spectral amplitudes with increasing frequency appears to be faster for the Yucca Flat shot than for the Shagan explosion whereas for Lg the reverse seems to be the case. For frequencies less than about 7 Hz, the spectral ratio Pn/Lg increases with frequency at a rate much faster for the Shagan explosion than for the Yucca Flat shot.

Average Pn/Lg amplitude ratios were computed for all 53 explosions, which included 21 BWT and 32 AWT shots. Plots of this ratio versus overburden velocity, work point velocity, and shot depth are shown in Figures 12a, 13a, and 14a, respectively for all 53, 21 BWT, and 32 AWT shots. In order to avoid possible complicated effects of proximity to the water table on regional phases (Blandford, 1976), the observed results were reexamined by excluding explosions with their shot points within one cavity radius of the water table. The cavity radii for various shots were computed by using Closmann's (1969) empirical relationships for shots with known yield and shot medium. The resulting plots for explosions that are either well below the water table (WBWT) or well above the water table (WAWT) are shown in Figures 12b, 13b, and 14b. An examination of the 18 least squares regressions shown in Figures 12 through 14 shows that the average ratio Pn/Lg generally increases with overburden velocity,

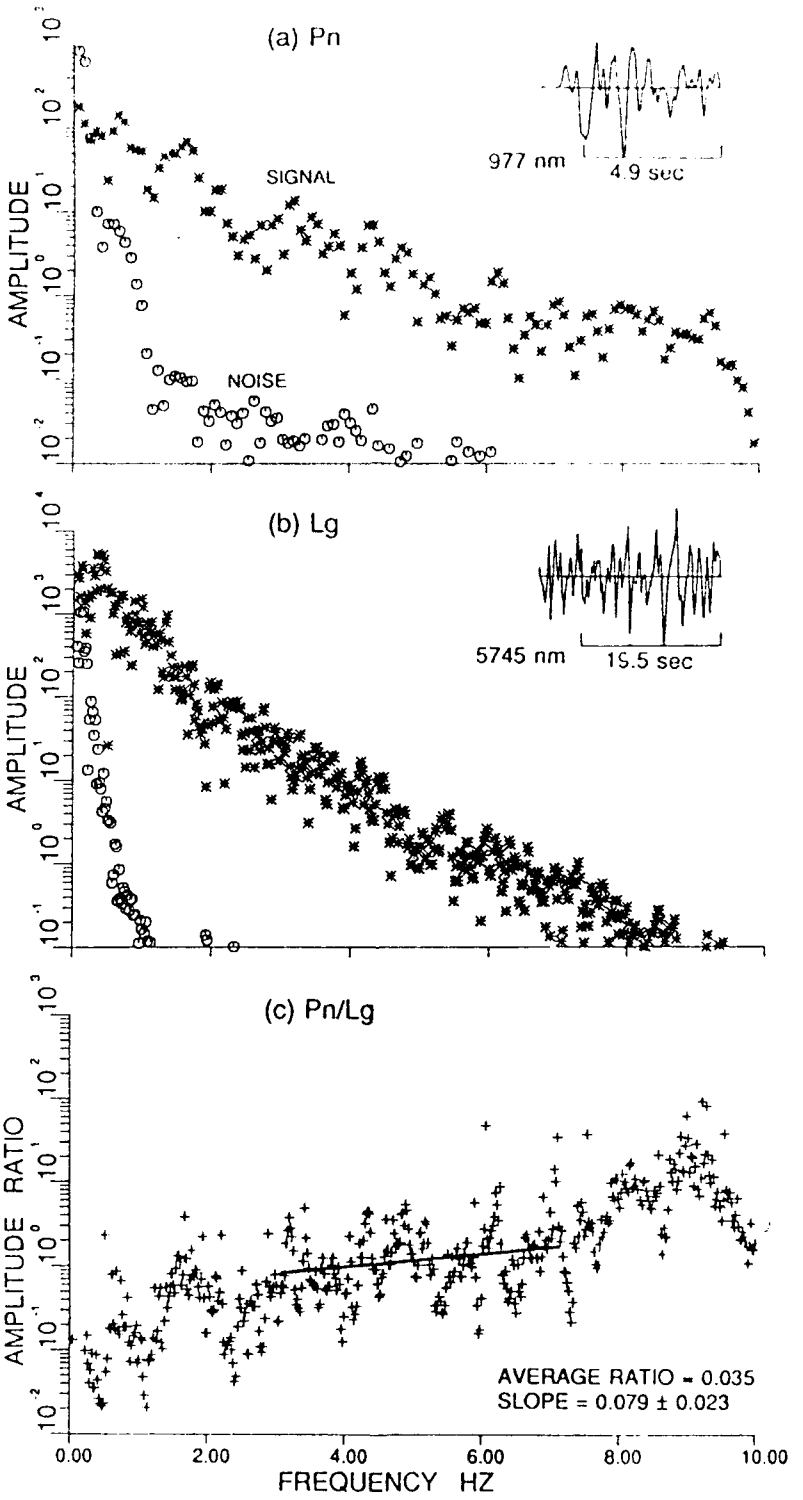

Figure 11. Similar to Figure 2 for the Yucca Flat explosion, ROUSANNE. A comparison of these results with those for the Shagan explosion in Figure 2 indicates large differences in both mean slope and average Pn/Lg amplitude ratio, over the frequency range 3-7 Hz.

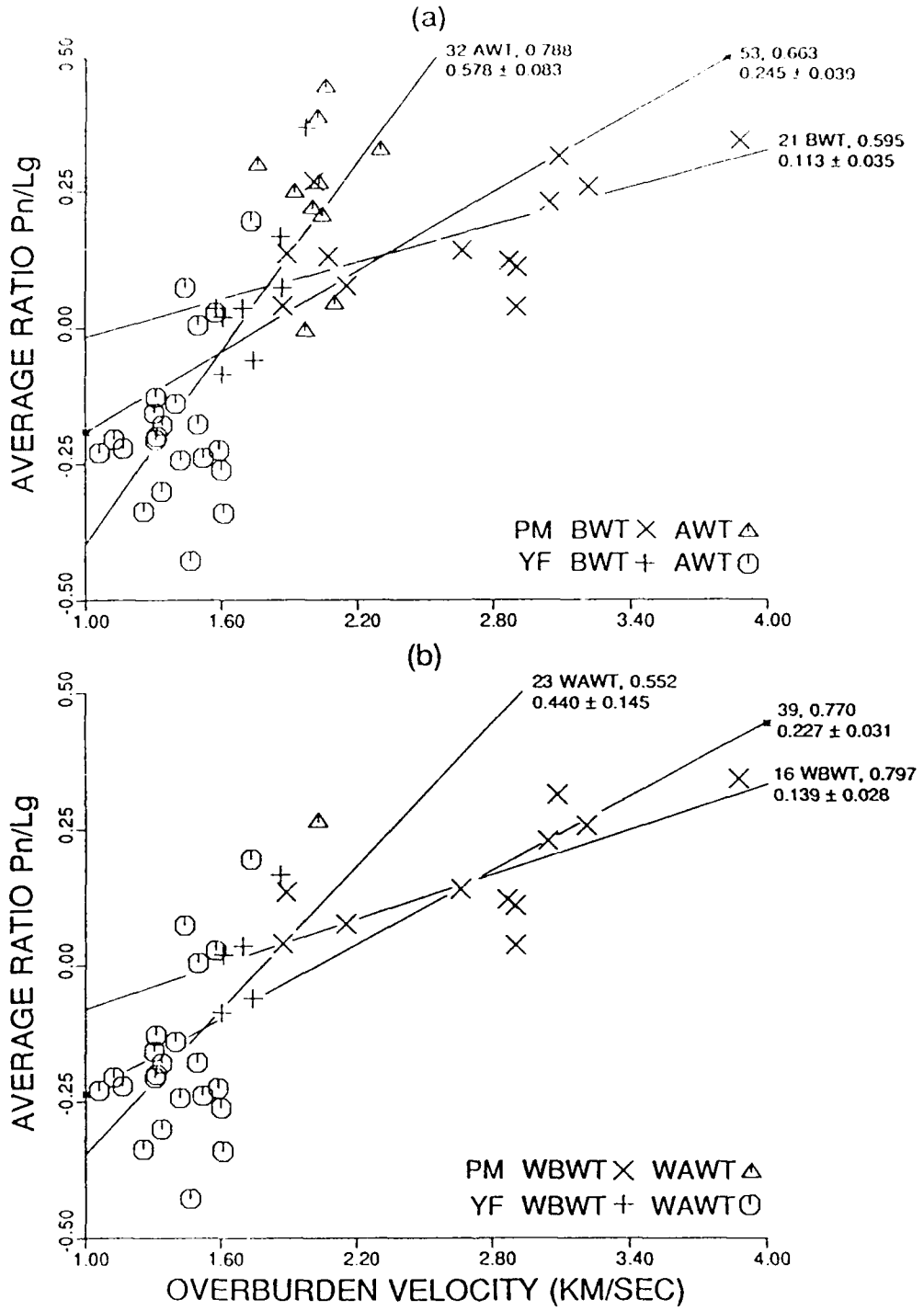

Figure 12. Average Pn/Lg amplitude ratio (in log units) for the frequency range of 3-7 Hz versus overburden velocity for (a) 53 explosions, including 21 BWT and 32 AWT shots, and (b) 39 shots with 16 well below water table (WBWT) and 23 well above water table (WAWT) shots. The number of explosions, correlation coefficient, and mean slope (with one standard deviation value) are indicated near each regression line. Note the general increase in the average ratio Pn/Lg with overburden velocity in all cases.

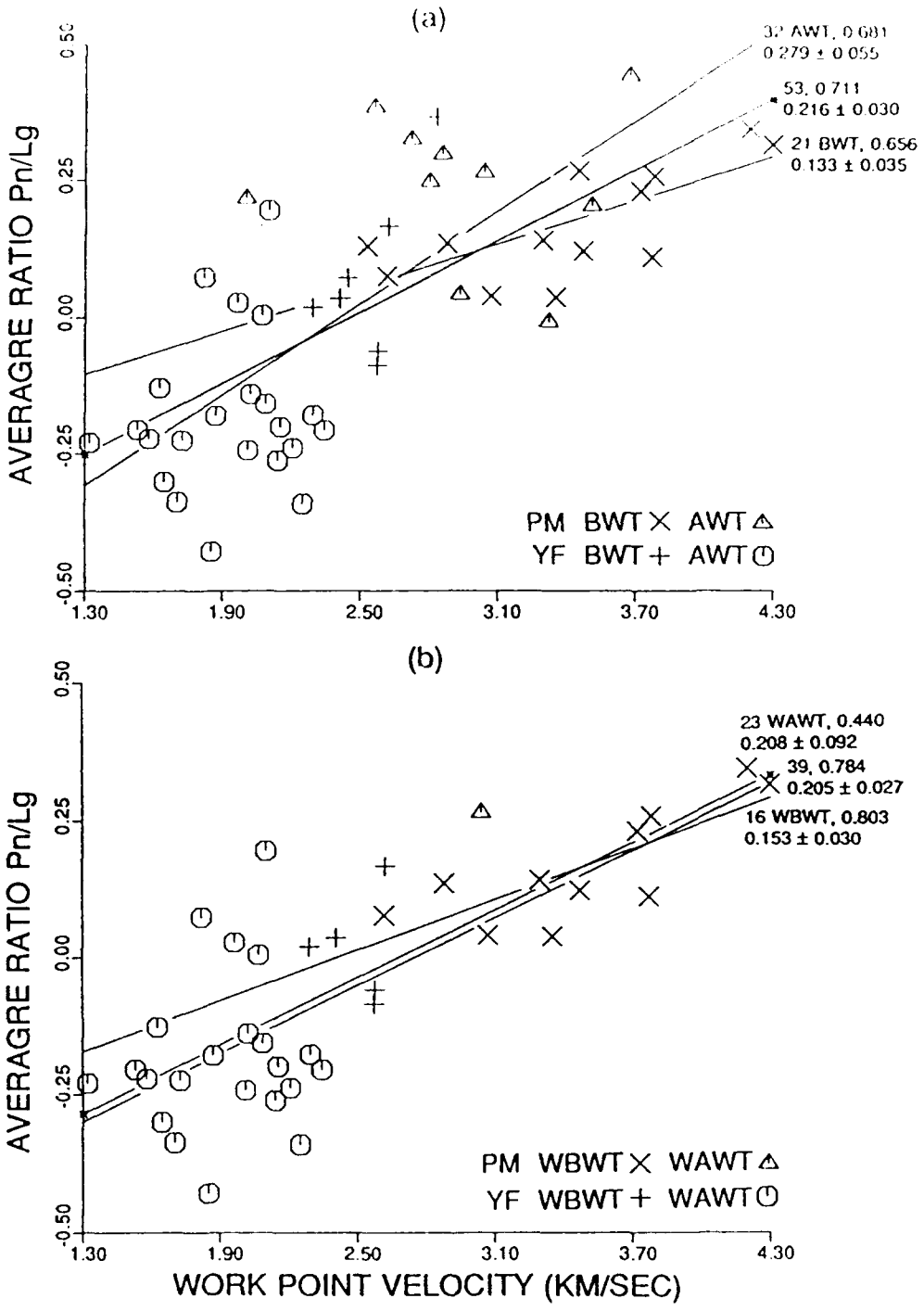

Figure 13. Similar to Figure 12 but for work point velocity. Regression results are similar to those in Figure 12 and indicate general increase in the average ratio Pn/Lg with work point velocity in all cases.

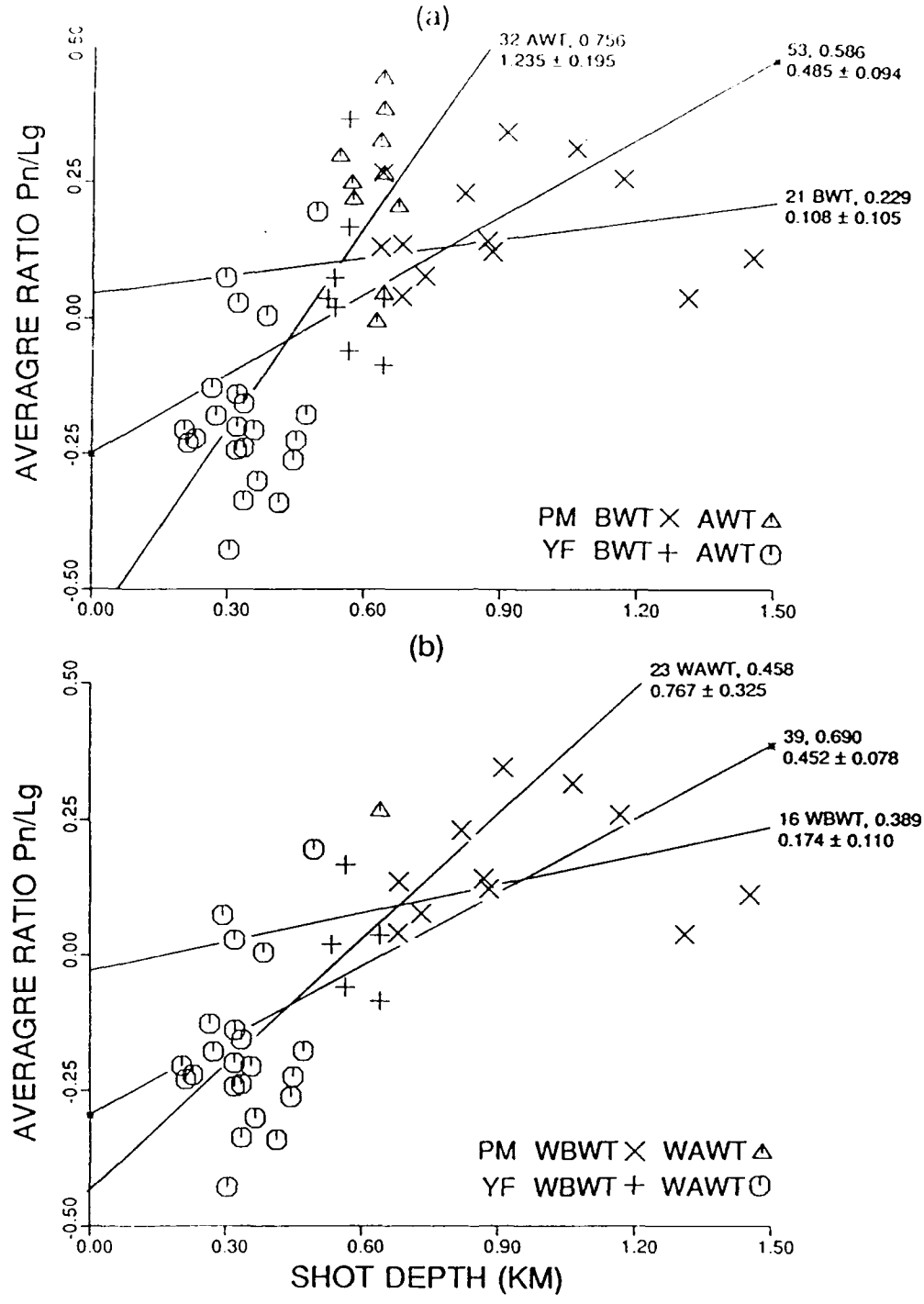

Figure 14. Similar to Figure 12 but for shot depth. Regression results indicate much weaker dependence than on overburden velocity (Figure 12) or work point velocity (Figure 13), especially for 21 BWT and 16 WBWT shots.

work point velocity, and shot depth. However, whereas Pn/Lg is influenced by the two velocities (overburden and work point) by nearly the same extent, there is considerably weaker dependence on shot depth, especially for BWT and WBWT shots. In a study of geophysical properties of shot media at NTS, Ramspott and Howard (1975) observed that, "of the various media, Yucca Flat and Pahute Mesa above the water table are the most variable. In these areas, it is possible to find individual past sites with extreme values of reported parameters. The other media are relatively uniform." This means that more weight or credibility should be given to results from BWT or WBWT shots for which the correlation coefficient values are nearly the same for regressions of Pn/Lg versus overburden velocity (Figure 12) and Pn/Lg versus work point velocity (Figure 13) but are considerably smaller for Pn/Lg versus shot depth (Figure 14). It appears therefore that medium velocity is the parameter that directly influences Pn/Lg and the apparent dependence on shot depth is only due to the correlation that generally exists between shot depth and medium velocity.

In order to study possible effect of gas porosity on the regional phases, average Pn/Lg amplitude ratios (3-7 Hz) for the same 53 shots were plotted versus gas porosity (Figure 15a). The regression results appear to suggest significant dependence which may, however, be due to the gas porosity being directly related to overburden velocity. To check this possibility, data from Yucca Flat shots which have large variations in both overburden velocity and gas porosity were selected. A plot of Pn/Lg for 30 Yucca Flat shots versus overburden velocity (Figure 15b) was used to obtain the corresponding Pn/Lg residuals which were then plotted versus gas porosity (Figure 15c). The weak dependence, as indicated by the extremely low correlation coefficient in Figure 15c, suggests that the difference between P and Lg amplitudes is insensitive to gas porosity when the data are corrected for the effect of overburden velocity.

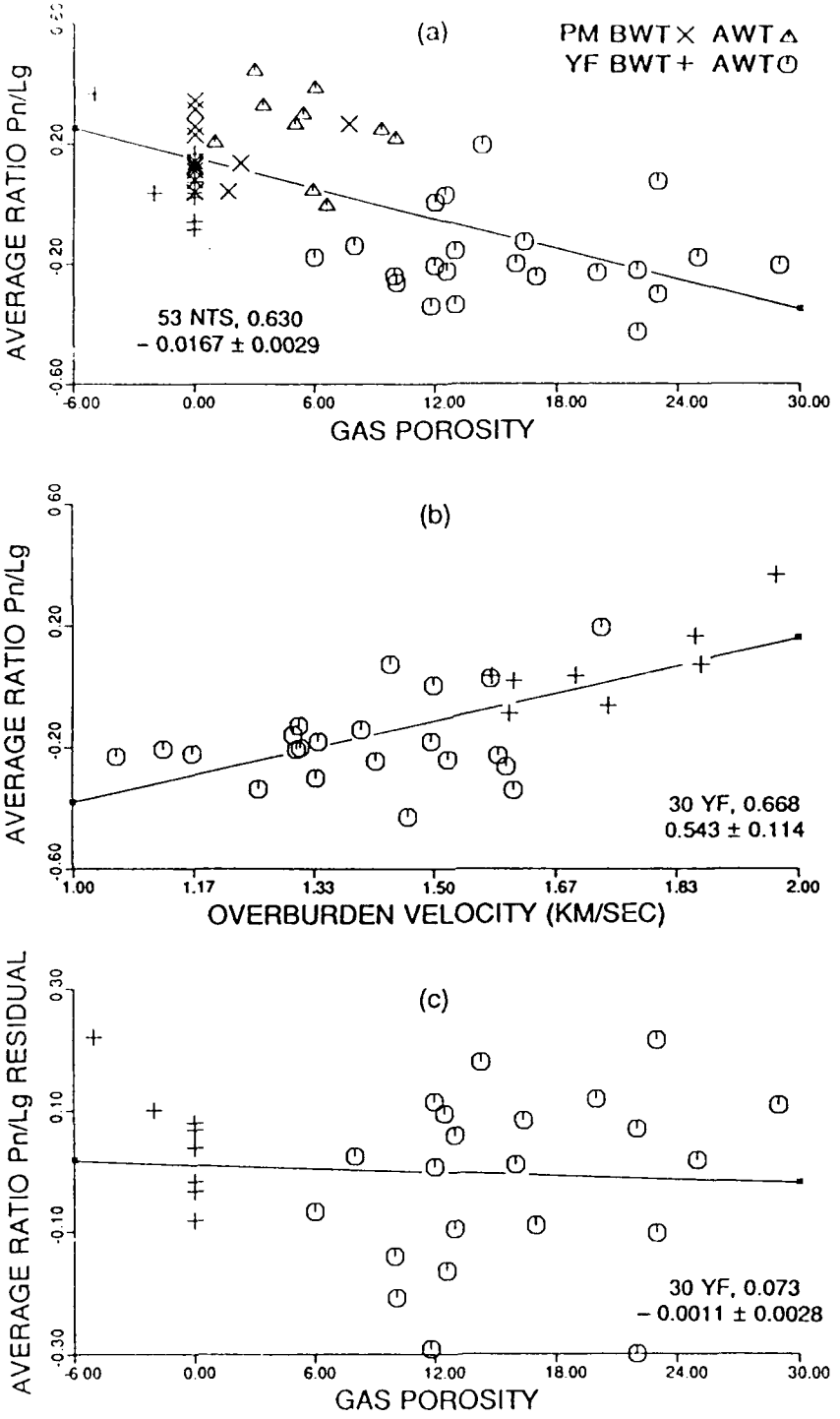

Figure 15. Similar to Figure 10 but for average ratio Pn/Lg (3-7 Hz) for 53 NTS shots. Again, the dependence on gas porosity is not significant when the data are corrected for the effect of overburden velocity.

A plot of the average Pn/Lg amplitude ratios for the same 53 explosions on a map of NTS (Figure 16a) shows that, for fixed Pn, the Yucca Flat explosions generally have considerably larger Lg than the Pahute Mesa shots. Figure 16b shows the corresponding variations in overburden velocity. Similarity between the two figures suggests good correlation between Pn/Lg and shot medium velocity, as was also indicated earlier in Figure 12.

An attempt was made to study the variation of Pn and Lg with m_b for NTS shots and compare the results with those for the USSR shots. From published Soviet yields, m_b = 6.0 corresponds to a yield of about 110 kt (Vergino, 1989). For NTS shots, an explosion with yield of 110 kt will have m_b of about 5.5 (e.g. Bache, 1982). The 23 Pahute Mesa explosions covered a rather small range of m_b and were therefore not used for this purpose. The same procedure as applied to the USSR shots was used to compute the RMS values for several frequency ranges for both Pn and Lg phases for the 30 Yucca Flat shots. The latter included 7 overburied shots with scaled depth, defined as (shot depth, m)/(yield, kt)$^{1/3}$, greater than 200 whereas the usual scaled depth for most NTS shots is about 120 m/kt$^{1/3}$ (Mueller and Murphy, 1971). Log RMS values were plotted versus m_b, where the latter are maximum-likelihood estimates of P. D. Marshall (written communication). Results for frequency bands of 0.5-1.0 Hz and 4.0-6.0 Hz are shown in Figure 17, in which the overburied and the BWT and AWT shots are identified. Most overburied shots appear to be outliers, especially at the higher frequency. Linear regressions were therefore performed on the 23 "normal" shots; the corresponding results are indicated in Figure 17. The mean slope for Lg is somewhat smaller than for Pn, especially for the higher frequency. Similar to Figure 5, for a fixed m_b, the reduction in RMS at the higher frequency is larger for Lg than for Pn. However, unlike the results from the USSR explosions in Figure 5, the higher frequency slopes are not much

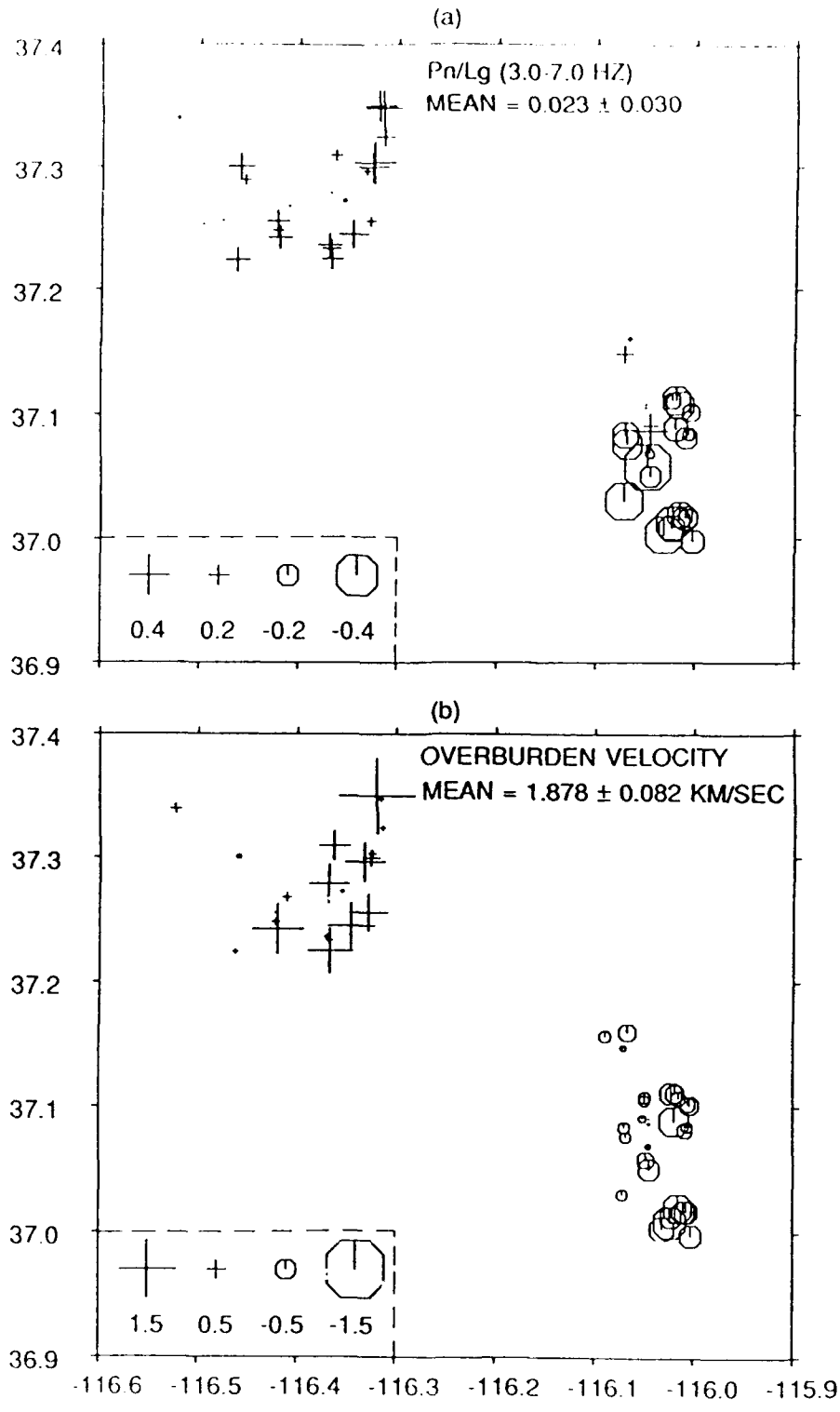

Figure 16. (a) Similar to Figure 4b for 53 NTS shots showing significant differences between Pahute Mesa and Yucca Flat explosions. (b) Corresponding overburden velocities, showing good correlation with the Pn/Lg amplitude ratios.

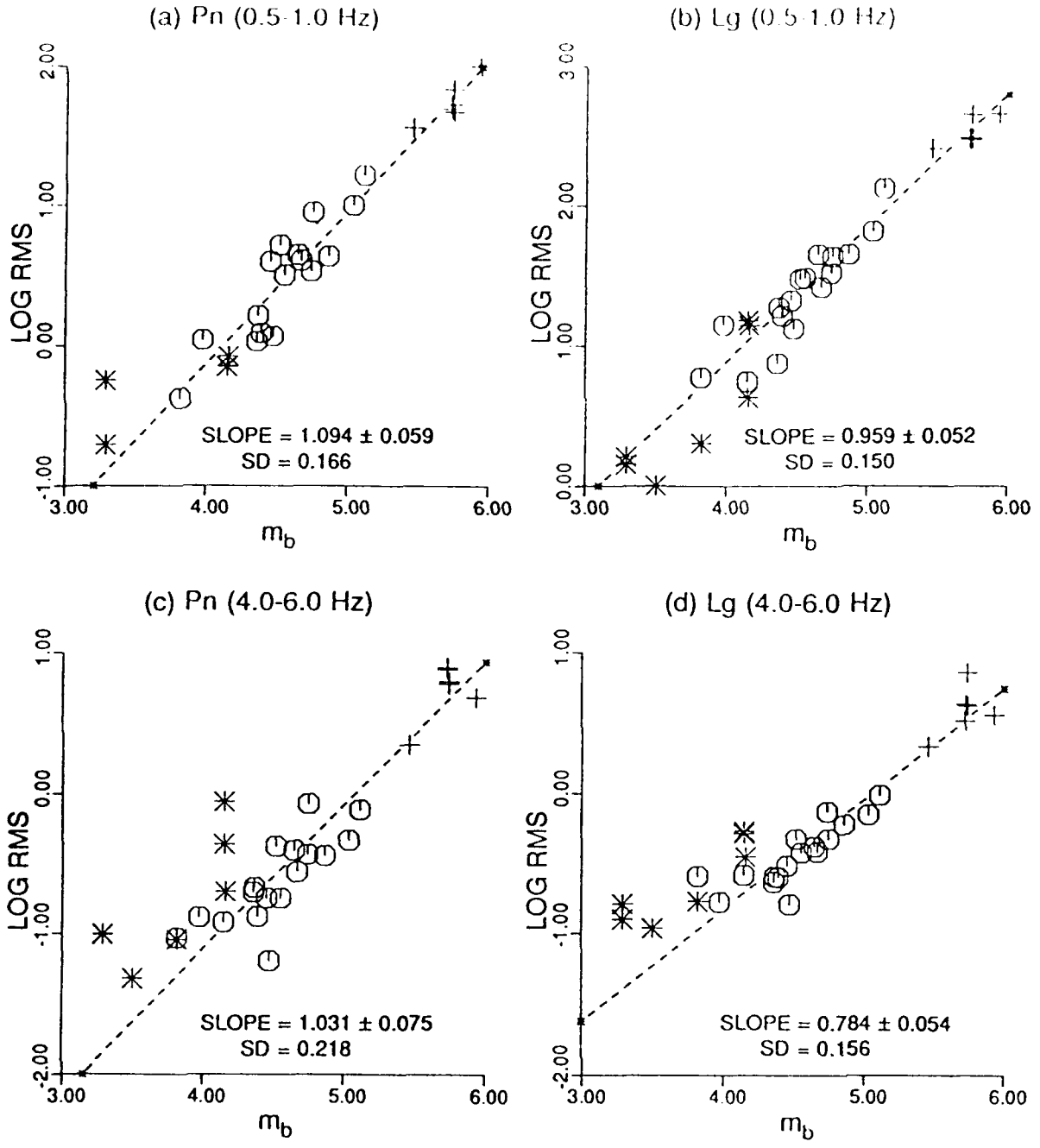

Figure 17. Similar to Figure 5 for 30 Yucca Flat explosions (including 7 overburied shots). Six BWT, 17 AWT and 7 overburied shots are denoted by the symbols +, o, and *, respectively. Regression results shown are for 23 "normal" shots.

different from the lower frequency slopes. In order to make sure that the results in Figure 17 are not due to possible errors in m_b, Pn and Lg RMS values were also plotted versus yield. The results, shown in Figure 18, are not substantially different from those in Figure 17. The Lg slopes are again smaller than those of Pn, more so for the higher frequency.

Plots of RMS versus m_b for Yucca Flat shots (such as those in Figure 17) were used to compute mean log RMS values of Pn and Lg for $m_b = 5.5$ for several frequency bands, in the same manner as for the USSR shots. Results for five center frequencies, shown in Figure 6, indicate Pn(RMS) and Lg (RMS) to vary by about 1 and 2 m.u., respectively, over the range of about 1-5 Hz. A comparison of Shagan and Yucca Flat data show vast differences in the frequency dependence of both Pn and Lg. In comparison to Pn(Yucca-Flat), Pn(Shagan) decreases very slowly with frequency, perhaps due to smaller attenuation of Pn in the shield region of the USSR as compared to the western United States. For low frequencies, Lg diminishes *more* rapidly with frequency for Shagan explosions than for Yucca Flat shots. In other words, Lg from Shagan explosions is relatively richer in lower frequencies than that from Yucca Flat shots.

Similar to the method used for the USSR shots, log RMS amplitude ratios Pn/Lg, computed separately for 23 Pahute Mesa and 30 Yucca Flat shots, were plotted versus m_b, and then linear regression was used to obtain the mean values for $m_b = 5.5$. Results for Pahute Mesa and Yucca Flat explosions, also included in Figure 7, indicate significant differences in the dependence of their Pn/Lg on frequency. A comparison of the four plots in Figure 7 shows that Pn/Lg for NTS shots increases with frequency at a rate that is significantly smaller than for the USSR shots. The P-wave velocities for Shagan and Degelen test sites, estimated as 5.5-6.0 km/sec and 3.5-4.5 km/sec, respectively (Bonham *et al.*, 1980), are considerably

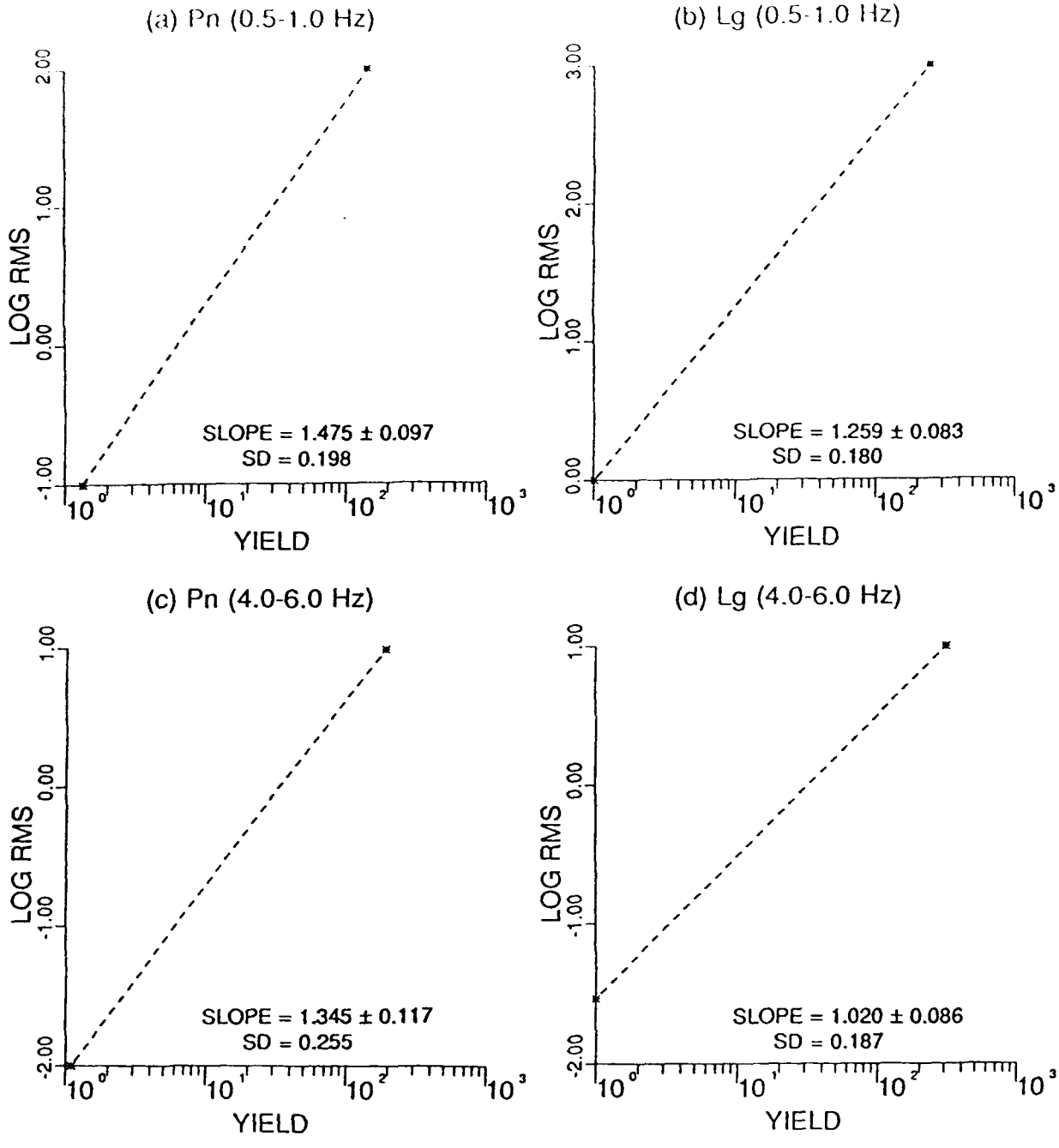

Figure 18. Similar to Figure 5 but for log yield (instead of m_b) for 23 Yucca Flat explosions. For each of the two frequency passbands, the mean slope for Lg is significantly smaller than that for Pn.

higher than those for NTS. Rock velocities for Pahute Mesa shots are generally higher than those for Yucca Flat explosions. For example, the average overburden velocities for BWT shots at Pahute Mesa and Yucca Flat test sites are 2.9 and 1.7 km/sec, respectively (Ramspott and Howard, 1975). Therefore, the four plots in Figure 7 indicate that, considering explosions of similar yield, the amplitude ratio Pn/Lg systematically increases with the source medium velocity and this dependence is stronger at higher frequencies.

DISCUSSION

Frankel (1989) investigated the effects of source depth and crustal structure on the spectra of regional Lg by analyzing synthetic seismograms. His results show that the low frequency (less than about 0.5 Hz) Lg is mainly due to S*. As long as the shot point P wave velocity is smaller than the S wave velocity below the Moho, most of the higher frequency Lg originates from the pS phase from the explosion. However, when the source region P wave velocity is greater than the S wave velocity below the Moho, the pS phase would not be trapped into the Lg phase, and Lg will be dominated by the lower frequency S*. His results for two different shot-point velocity values (4.5 and 5.0 km/sec) for a crustal model in which the S-wave velocity below the Moho is 4.5 km/sec are shown in Figure 19. The source-receiver distance is 300 km. The effect of variations in shot depth (500 m and 1500 m) is minimal whereas, at the higher frequencies, the lower velocity medium has considerably larger Lg than the higher velocity medium. The shot point velocity influences the degree to which pS is trapped, whereas the overburden velocity controls the generation of S*. The seismic velocity structure in the Eastern Kazakh region indicates a velocity of about 5.4 km/sec in the uppermost 5 km of the crust, and the S-wave velocity below the Moho is about 4.7 km/sec (William Leith, written communication, 1989). One may therefore expect the Lg spectra of explosions at NTS and East Kazakh to be somewhat similar to those in Figures 19a and 19b, respectively.

Since larger m_b implies greater shot depth, our results (Figures 3, 9, and 14) indicate Lg to be nearly independent of shot depth, in agreement with the theoretical results in Figure 19. The observed reduction in amplitudes with frequency is considerably larger for Lg than for Pn

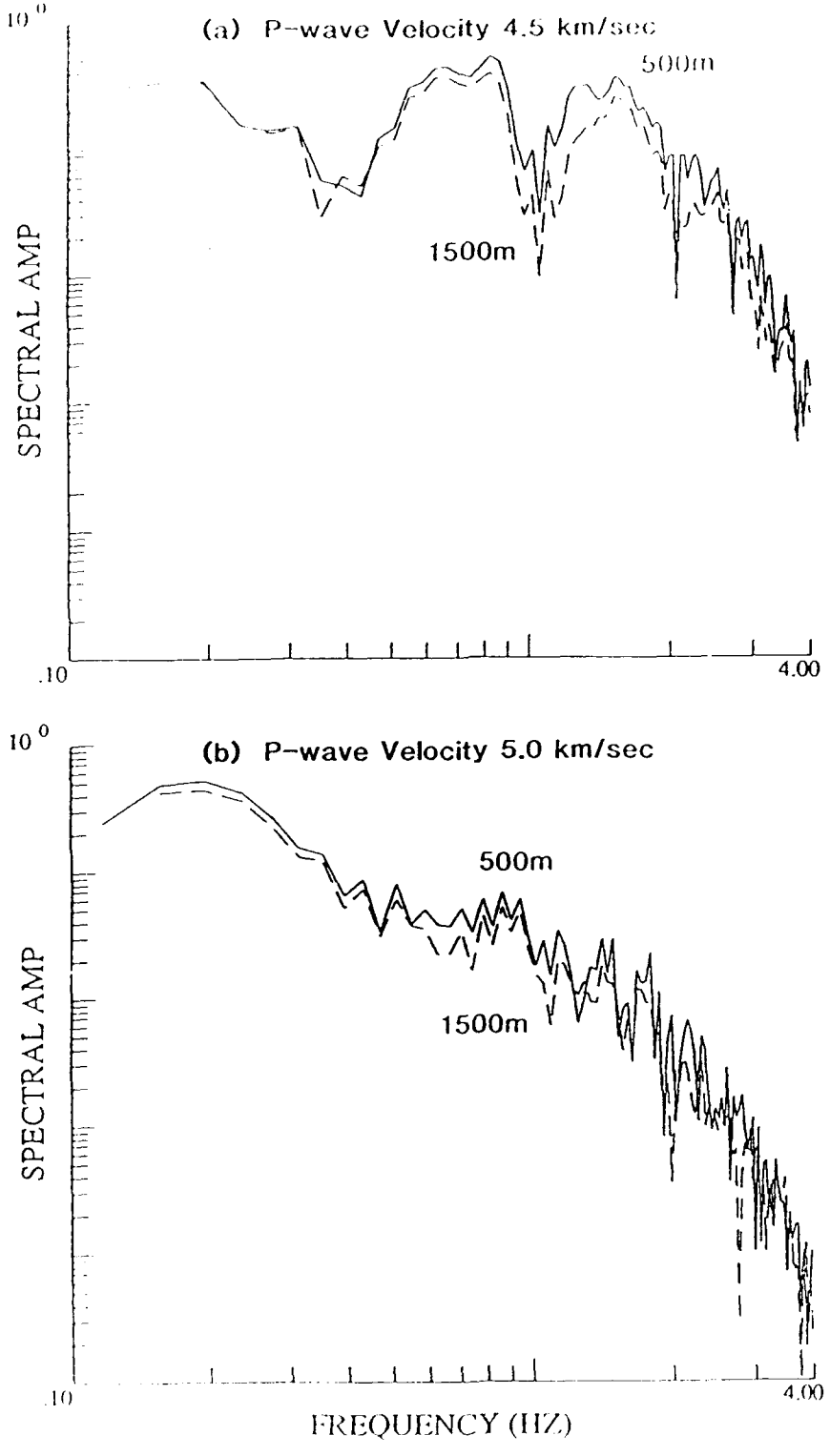

Figure 19. Lg spectra for explosions at 500m and 1500m depth with P-wave velocity in the source layer of (a) 4.5 km/sec and (b) 5.0 km/sec (after Frankel, 1989). The effect of large variation in shot depths is minimal whereas a small change in source layer velocity has significant effect on spectra at the higher frequencies.

for East Kazakh as well as for NTS shots (Figure 6). For frequencies less than about 2 Hz, Lg diminishes more rapidly with frequency for the USSR shots than for the NTS shots and, for the higher frequencies, at about the same rate, again in agreement with Figure 19. The observed rapid increase of Pn/Lg with frequency for the USSR shots (Figure 7) is therefore likely to be due to the local crustal structure which makes Lg dominated by S*. For the NTS shots, the smaller rates of increase of Pn/Lg with frequency are probably due to P-wave velocities in the uppermost layers that are considerably smaller than the S-wave velocity below the Moho so that Lg originates mainly from the explosion pS.

Analysis of both East Kazakh and NTS explosion data has indicated the difference between Pn and Lg amplitudes to be insensitive to shot depth, except through its relationship with medium velocity. Based on the analysis of NTS data, the same is true of gas porosity. Note that Patton (1988) observed the same dependence of gas porosity on both $m_b(P)$ and $m_b(Lg)$, and so $m_b(P) - m_b(Lg)$ or the amplitude ratio Pn/Lg does not depend on gas porosity.

The Pn(RMS) versus m_b plots in Figure 17 do not indicate any reduction in the mean slope at the higher frequency, observed for the Shagan explosions (Figure 5) and expected on the basis of source scaling. A possible reason is that whereas all Shagan explosions are detonated below the water table, the Yucca Flat shots include both BWT and AWT shots, and the former are of larger m_b than the latter. In comparing the spectral characteristics of BWT and AWT shots, Gupta *et al.* (1989b) observed that for the same low-frequency spectral level, BWT shots had somewhat higher corner frequencies than AWT shots. This means that for the same m_b, BWT shots may be relatively richer in the higher frequencies so that, for the data in Figure 17c, the enhanced amplitudes of BWT shots will tend to increase the mean slope, as observed. At the higher frequency, the mean slope for Lg (Figure 17d) is

considerably smaller than for Pn (Figure 17c), probably because of the greater excitation of Lg for the smaller m_b, lower velocity shots (see Figures 12 and 13).

Spatial attenuation of Pn and Lg will no doubt affect the observed spectra and the spectral ratios Pn/Lg derived in this study. Unfortunately, Q values for correcting the observed spectra, especially at the higher frequencies, are not available and the appropriate corrections cannot be made. For the western U.S., Bakun and Johnson (1970) estimated Q(Pn) to be about 400, whereas for Lg Chavez and Priestley (1986) gave the relationship $Q(f) = 206\ f^{0.68}$. For the East Kazakh region, Sereno (1990) estimated Q(Pn) and Q(Lg) for frequency ranges of 1 to 10 Hz and 0.5 to 2.5 Hz, respectively. His results for Lg indicate Q(f) between $500\ f^{0.19}$ and a constant value of 650; Q(f) for Pn is not as well-constrained but may lie between $300\ f^{0.5}$ and a constant value of 1175. For Lg in the Eastern Kazakh region, Priestley *et al.* (1990) obtained $Q(f) = 367\ f^{0.48}$, whereas Given *et al.* (1990) derived a frequency-dependent value of $500\ f^{0.5}$. It follows that although there is considerable uncertainty in the attenuation parameters, Q(Pn) as well as Q(Lg) for East Kazakh are about 2 to 3 times those for WUS, at least for frequency of about 1 Hz. Since the source-receiver distance for East Kazakh shots is about 2.4 times that for the NTS shots, the effects of attenuation on Pn and Lg phases will be nearly the same for East Kazakh and NTS shots. However, this may not be true at the higher frequencies for which precise Q values are not available. Therefore, it seems that our conclusions regarding the differences in the excitation of Pn and Lg from USSR and NTS shots are not significantly influenced by attenuation.

Gupta and Blandford's (1987) analysis of teleseismic P arrivals from NTS shots showed the P/P-coda spectral *slope* (0.5-3.0 Hz) to increase with shot medium velocity. Their results also implied that, at *higher frequencies*, the *amplitude* ratio P/P-coda is larger for shot media

with higher velocity. Thus the amplitude ratios Pn/Lg derived from regional data and P/P-coda obtained from teleseismic data show similar dependence on shot medium velocity. Teleseismic P coda is generally believed to be due to both near-source and near-receiver scattering involving S to teleseismic P and teleseismic P to S conversions, respectively (Dainty, 1990). Therefore, a possible explanation for our observations is that shots in lower velocity media somehow generate larger amounts of high frequency S waves (than those in higher velocity media) which contribute directly to Lg and, by near-source scattering, to P coda. Alternatively, there could be larger near-source scattering of S into teleseismic P for lower velocity media, for which greater high frequency Lg is also expected from theory (see Figure 19). However, it is not clear how the generation and/or scattering of high frequency S would depend on the shot medium velocity.

Our results demonstrating the observed Lg spectra to vary systematically with medium velocity appear to suggest that S* is mainly responsible for the low-frequency Lg from nuclear explosions at both East Kazakh and Nevada test sites. Perhaps the scattering of explosion-generated Rg into P and S waves also contributes to the low-frequency Lg, especially for the NTS explosions (Stead and Helmberger, 1989; Gupta *et al.*, 1990). Taylor and Randall (1989) suggested that spall has a significant effect on the regional phases Pn and Pg. McLaughlin (1990) also proposed that spall, defined as nonlinear free-surface interaction, is responsible for the generation of low-frequency S waves (including Lg) and low-frequency P phases (Pn and Pg). More detailed studies of regional phases are needed to resolve these differences and understand the individual roles of S*, spall, and any other sources of shear wave energy from nuclear explosions.

CONCLUSIONS

An understanding of the generation and propagation of regional phases within the USSR is essential for the detection, source discrimination, and yield determination of Soviet underground nuclear explosions. Our comparison of the spectral characteristics of regional phases Pn and Lg from East Kazakh and NTS, with vastly different near-surface crustal structures, has provided useful information regarding the role of near-source environment, especially for the shot medium velocity. Analysis of Pn and Lg phases from the CDSN station WMQ suggests significant differences in the relative excitation of Pn and Lg between Shagan and Degelen test sites. For both East Kazakh and NTS shots, the reduction of amplitude with frequency is considerably larger for Lg than for Pn. For explosions of similar yield, the amplitude ratio Pn/Lg increases with frequency at a rate that appears to vary directly with the source medium velocity. At higher frequencies, the amplitude ratio Pn/Lg shows significant differences between USSR and NTS explosions, and these differences seem to be due to the large difference in the shot media velocities. The observed strong dependence of Lg spectra on medium velocity can be explained on the basis of contributions of pS and S* expected from theory. Lg from East Kazakh explosions appears to be dominated by S*, whereas that from NTS shots includes contributions from both pS and S*.

ACKNOWLEDGMENTS

We thank Robert R. Blandford, Art Frankel, and Bill Leith for valuable advice and suggestions during the course of this study. This research was funded by the Defense Advanced Research Projects Agency and monitored by the Geophysics Laboratory under Contract F19628-88-C-0051. The views and conclusions contained in this report are those of the authors and should not be interpreted as necessarily representing the official policies, either expressed or implied, of the Defense Advanced Research Projects Agency or the U. S. Government.

REFERENCES

Bache, T. C. (1982). Estimating the yield of underground nuclear explosions, *Bull. Seism. Soc. Am. 72,* S131-S168.

Bakun, W. H. and L. R. Johnson (1970). Short period spectral discriminants for explosions, *Geophys. J. R. Astr. Soc. 22,* 139-152.

Blandford, R. R. (1976). Experimental determination of scaling laws for contained and cratering explosions, *SDAC-TR-76-3,* Teledyne Geotech, Alexandria, Virginia.

Bonham, S., W. J. Dempsey, and J. Rachlin (1980). Geologic environment of the Semipalatinsk area, U.S.S.R. *(Preliminary Report),* U. S. Geological Survey, Reston, Virginia.

Chavez, D. E. and K. F. Priestley (1986). Measurement of frequency dependent Lg attenuation in the Great Basin, *Geophys. Res. Lett. 13,* 551-554.

Closmann, P. J. (1969). On the prediction of cavity radius produced by an underground nuclear explosion, *J. Geophys. Res. 74,* 3935-3939.

Dainty, A. (1990). Studies of coda using array and three-component processing, *PAGEOPH 132 (1-2),* 221-244.

Frankel, A. (1989). Effects of source depth and crustal structure on the spectra of regional phases determined from synthetic seismograms, *DARPA/AFTAC Annual Seismic Research Review,* 97-118, Patrick Air Force Base, Florida.

Given, H., N. Tarasov, V. Zhuravlev, F. Vernon, J. Berger, and I. Nersesov (1990). High-frequency seismic observations in eastern Kazakhstan, USSR, with emphasis on chemical explosion experiments, *J. Geophys. Res. 95,* (in press).

Gupta, I. N., B. W. Barker, J. A. Burnetti, and Z. A. Der (1970). A study of regional phases from earthquakes and explosions in Western Russia, *Bull. Seism. Soc. Am. 70,* 851-872.

Gupta, I. N. and R. R. Blandford (1983). A mechanism for generation of short-period transverse motion from explosions, *Bull. Seism. Soc. Am. 73,* 571-591.

Gupta, I. N. and R. R. Blandford (1987). A study of P waves from Nevada Test Site explosions: near-source information from teleseismic observations?, *Bull. Seism. Soc. Am. 77,* 1041-1056.

Gupta, I. N., R. S. Jih, and R. A. Wagner (1989a). Effect of depth and other physical parameters on P and Lg magnitude-yield relationships, *Paper presented at* DARPA/AFTAC Annual Seismic Research Review, Patrick Air Force Base, Florida.

Gupta, I. N., C. S. Lynnes, W. W. Chan, and R A. Wagner (1989b). A comparison of the spectral characteristics of nuclear explosions detonated below and above the water table, *GL-TR-89-0151*, Geophysics Laboratory, Hanscom Air Force Base, Massachusetts. ADA 214595.

Gupta, I. N., C. S. Lynnes, T. W. McElfresh, and R. A. Wagner (1990). F-k analysis of NORESS array and single-station data to identify sources of near-receiver and near-source scattering, *Bull. Seism. Soc. Am. 80*, (October).

Gutowski, P. R., F. Hron, D. E. Wagner, and S. Treitel (1984). S*, *Bull. Seism. Soc. Am. 74*, 61-78.

Kennett, B. L. N. (1989). On the nature of regional seismic phases - I. Phase representations for Pn, Pg, Sn, Lg, *Geophys. J. 98*, 447-456.

Lilwall, R. C. (1988). Regional m_b:M_s, *Lg/Pg* amplitude ratios and Lg spectral ratios as criteria for distinguishing between earthquakes and explosions: a theoretical study, *Geophys. J. 93*, 137-147.

McLaughlin, K. L. (1990). Excitation of Lg and P coda by shallow seismic sources, *Seismol. Res. Lett. 61*, 12.

Mueller, R. A. and J. R. Murphy (1971). Seismic characteristics of underground nuclear detonations, *Bull. Seism. Soc. Am. 61*, 1675-1692.

Murphy, J. R. and T. J. Bennett (1982). A discrimination analysis of short-period regional seismic data recorded at Tonto Forest Observatory, *Bull. Seism. Soc. Am. 72*, 1351-1366.

Patton, H. J. (1987). Yield estimation and the application of Nuttli's method to NTS explosions recorded on LLNL's Digital Seismic System (U), *UCID-21128*, Lawrence Livermore National Laboratory, Livermore, California.

Patton, H. J. (1988). Application of Nuttli's method to estimate yield of Nevada Test Site explosions recorded on Lawrence Livermore National Laboratory's digital seismic system, *Bull. Seism. Soc. Am. 78*, 1759-1772.

Priestley, K. F., W. R. Walter, V. Martynov, and M. V. Rozhkov (1990). Regional seismic recordings of the Soviet nuclear explosion of the Joint Verification Experiment, *Geophys. Res. Lett. 17*, 179-182.

Ramspott, L. D. and N. W. Howard (1975). Average properties of nuclear test areas and media at the USERDA Nevada Test Site, *UCRL-51948*, Lawrence Livermore Laboratory, Livermore, California.

Ringdal, F. and J. Fyen (1988). Comparative analysis of NORSAR and Grafenberg Lg magnitudes for Shagan River explosions, *NORSAR Scientific Rep. 1-88/89*, 88-103, Kjeller, Norway.

Ringdal, F. and P. D. Marshall (1989). Yield determination of Soviet underground nuclear explosions at the Shagan River test site, NORSAR Scientific Rep. 2-88/89, 36-67, Kjeller, Norway.

Sereno, T. J. Jr. (1990). Frequency-dependent attenuation in Eastern Kazakhstan and implications for seismic detection thresholds in the Soviet Union, *Paper presented at* Symposium on Regional Seismic Arrays and Nuclear Test Ban Verification, Oslo, Norway, 14-17 February 1990.

Stead, R. J. and D. V. Helmberger (1988). Numerical-analytical interfacing in two dimensions with applications to modeling NTS seismograms, *PAGEOPH 128, Nos. 1/2,* 157-193.

Taylor, S. R. and G. E. Randall (1989). The effects of spall on regional seismograms, *Geophys. Res. Lett. 16,* 211-214.

Vergino, E. S. (1989). Soviet test yields, *EOS (Trans. Am. Geophys. Union) 70,* 1511-1525.

CONTRACTORS (United States)

Prof. Thomas Ahrens
Seismological Lab, 252-21
Division of Geological & Planetary Sciences
California Institute of Technology
Pasadena, CA 91125

Prof. Charles B. Archambeau
CIRES
University of Colorado
Boulder, CO 80309

Dr. Thomas C. Bache, Jr.
Science Applications Int'l Corp.
10260 Campus Point Drive
San Diego, CA 92121 (2 copies)

Prof. Muawia Barazangi
Institute for the Study of the Continent
Cornell University
Ithaca, NY 14853

Dr. Douglas R. Baumgardt
ENSCO, Inc
5400 Port Royal Road
Springfield, VA 22151-2388

Prof. Jonathan Berger
IGPP, A-025
Scripps Institution of Oceanography
University of California, San Diego
La Jolla, CA 92093

Dr. Lawrence J. Burdick
Woodward-Clyde Consultants
566 El Dorado Street
Pasadena, CA 91109-3245

Dr. Karl Coyner
New England Research, Inc.
76 Olcott Drive
White River Junction, VT 05001

Prof. Vernon F. Cormier
Department of Geology & Geophysics
U-45, Room 207
The University of Connecticut
Storrs, CT 06268

Professor Anton W. Dainty
Earth Resources Laboratory
Massachusetts Institute of Technology
42 Carleton Street
Cambridge, MA 02142

Prof. Steven Day
Department of Geological Sciences
San Diego State University
San Diego, CA 92182

Dr. Zoltan A. Der
ENSCO, Inc.
5400 Port Royal Road
Springfield, VA 22151-2388

Prof. John Ferguson
Center for Lithospheric Studies
The University of Texas at Dallas
P.O. Box 830688
Richardson, TX 75083-0688

Prof. Stanley Flatte
Applied Sciences Building
University of California
Santa Cruz, CA 95064

Dr. Alexander Florence
SRI International
333 Ravenswood Avenue
Menlo Park, CA 94025-3493

Prof. Stephen Grand
University of Texas at Austin
Department of Geological Sciences
Austin, TX 78713-7909

Prof. Henry L. Gray
Vice Provost and Dean
Department of Statistical Sciences
Southern Methodist University
Dallas, TX 75275

Dr. Indra Gupta
Teledyne Geotech
314 Montgomery Street
Alexandria, VA 22314

Prof. David G. Harkrider
Seismological Laboratory
Division of Geological & Planetary Sciences
California Institute of Technology
Pasadena, CA 91125

Prof. Donald V. Helmberger
Seismological Laboratory
Division of Geological & Planetary Sciences
California Institute of Technology
Pasadena, CA 91125

Prof. Eugene Herrin
Institute for the Study of Earth and Man
GeophysicalLaboratory
Southern Methodist University
Dallas, TX 75275

Prof . Robert B. Herrmann
Department of Earth & Atmospheric Sciences
St. Louis University
St. Louis, MO 63156

Prof. Bryan Isacks
Cornell University
Department of Geological Sciences
SNEE Hall
Ithaca, NY 14850

Dr. Rong-Song Jih
Teledyne Geotech
314 Montgomery Street
Alexandria, VA 22314

Prof. Lane R. Johnson
Seismographic Station
University of California
Berkeley, CA 94720

Prof. Alan Kafka
Department of Geology & Geophysics
Boston College
Chestnut Hill, MA 02167

Dr. Richard LaCoss
MIT-Lincoln Laboratory
M-200B
P. O. Box 73
Lexington, MA 02173-0073 (3 copies)

Prof Fred K. Lamb
University of Illinois at Urbana-Champaign
Department of Physics
1110 West Green Street
Urbana, IL 61801

Prof. Charles A. Langston
Geosciences Department
403 Deike Building
The Pennsylvania State University
University Park, PA 16802

Prof. Thorne Lay
Institute of Tectonics
Earth Science Board
University of California, Santa Cruz
Santa Cruz, CA 95064

Prof. Arthur Lerner-Lam
Lamont-Doherty Geological Observatory
of Columbia University
Palisades, NY 10964

Dr. Christopher Lynnes
Teledyne Geotech
314 Montgomery Street
Alexandria, VA 22314

Prof. Peter Malin
University of California at Santa Barbara
Institute for Crustal Studies
Santa Barbara, CA 93106

Dr. Randolph Martin, III
New England Research, Inc.
76 Olcott Drive
White River Junction, VT 05001

Dr. Gary McCartor
Mission Research Corporation
735 State Street
P.O. Drawer 719
Santa Barbara, CA 93102 (2 copies)

Prof. Thomas V. McEvilly
Seismographic Station
University of California
Berkeley, CA 94720

Dr. Keith L. McLaughlin
S-CUBED
A Division of Maxwell Laboratory
P.O. Box 1620
La Jolla, CA 92038-1620

Prof. William Menke
Lamont-Doherty Geological Observatory
of Columbia University
Palisades, NY 10964

Stephen Miller
SRI International
333 Ravenswood Avenue
Box AF 116
Menlo Park, CA 94025-3493

Prof. Bernard Minster
IGPP, A-025
Scripps Institute of Oceanography
University of California, San Diego
La Jolla, CA 92093

Prof. Brian J. Mitchell
Department of Earth & Atmospheric Sciences
St. Louis University
St. Louis, MO 63156

Mr. Jack Murphy
S-CUBED, A Division of Maxwell Laboratory
11800 Sunrise Valley Drive
Suite 1212
Reston, VA 22091 (2 copies)

Dr. Bao Nguyen
GL/LWH
Hanscom AFB, MA 01731-5000

Prof. John A. Orcutt
IGPP, A-025
Scripps Institute of Oceanography
University of California, San Diego
La Jolla, CA 92093

Prof. Keith Priestley
University of Cambridge
Bullard Labs, Dept. of Earth Sciences
Madingley Rise, Madingley Rd.
Cambridge CB3 OEZ, ENGLAND

Prof. Paul G. Richards
L-210
Lawrence Livermore National Laboratory
Livermore, CA 94550

Dr. Wilmer Rivers
Teledyne Geotech
314 Montgomery Street
Alexandria, VA 22314

Prof. Charles G. Sammis
Center for Earth Sciences
University of Southern California
University Park
Los Angeles, CA 90089-0741

Prof. Christopher H. Scholz
Lamont-Doherty Geological Observatory
of Columbia University
Palisades, NY 10964

Thomas J. Sereno, Jr.
Science Application Int'l Corp.
10260 Campus Point Drive
San Diego, CA 92121

Prof. David G. Simpson
Lamont-Doherty Geological Observatory
of Columbia University
Palisades, NY 10964

Dr. Jeffrey Stevens
S-CUBED
A Division of Maxwell Laboratory
P.O. Box 1620
La Jolla, CA 92038-1620

Prof. Brian Stump
Institute for the Study of Earth & Man
Geophysical Laboratory
Southern Methodist University
Dallas, TX 75275

Prof. Jeremiah Sullivan
University of Illinois at Urbana-Champaign
Department of Physics
1110 West Green Street
Urbana, IL 61801

Prof. Clifford Thurber
University of Wisconsin-Madison
Department of Geology & Geophysics
1215 West Dayton Street
Madison, WS 53706

Prof. M. Nafi Toksoz
Earth Resources Lab
Massachusetts Institute of Technology
42 Carleton Street
Cambridge, MA 02142

Prof. John E. Vidale
University of California at Santa Cruz
Seismological Laboratory
Santa Cruz, CA 95064

Prof. Terry C. Wallace
Department of Geosciences
Building #77
University of Arizona
Tucson, AZ 85721

Dr. Raymond Willeman
GL/LWH
Hanscom AFB, MA 01731-5000

Dr. Lorraine Wolf
GL/LWH
Hanscom AFB, MA 01731-5000

OTHERS (United States)

Dr. Monem Abdel-Gawad
Rockwell International Science Center
1049 Camino Dos Rios
Thousand Oaks, CA 91360

Prof. Keiiti Aki
Center for Earth Sciences
University of Southern California
University Park
Los Angeles, CA 90089-0741

Prof. Shelton S. Alexander
Geosciences Department
403 Deike Building
The Pennsylvania State University
University Park, PA 16802

Dr. Kenneth Anderson
BBNSTC
Mail Stop 14/1B
Cambridge, MA 02238

Dr. Ralph Archuleta
Department of Geological Sciences
University of California at Santa Barbara
Santa Barbara, CA 93102

J. Barker
Department of Geological Sciences
State University of New York
at Binghamton
Vestal, NY 13901

Dr. T.J. Bennett
S-CUBED
A Division of Maxwell Laboratory
11800 Sunrise Valley Drive, Suite 1212
Reston, VA 22091

Mr. William J. Best
907 Westwood Drive
Vienna, VA 22180

Dr. N. Biswas
Geophysical Institute
University of Alaska
Fairbanks, AK 99701

Dr. G.A. Bollinger
Department of Geological Sciences
Virginia Polytechnical Institute
21044 Derring Hall
Blacksburg, VA 24061

Dr. Stephen Bratt
Center for Seismic Studies
1300 North 17th Street
Suite 1450
Arlington, VA 22209

Michael Browne
Teledyne Geotech
3401 Shiloh Road
Garland, TX 75041

Mr. Roy Burger
1221 Serry Road
Schenectady, NY 12309

Dr. Robert Burridge
Schlumberger-Doll Research Center
Old Quarry Road
Ridgefield, CT 06877

Dr. Jerry Carter
Rondout Associates
P.O. Box 224
Stone Ridge, NY 12484

Dr. W. Winston Chan
Teledyne Geotech
314 Montgomery Street
Alexandria, VA 22314-1581

Dr. Theodore Cherry
Science Horizons, Inc.
710 Encinitas Blvd., Suite 200
Encinitas, CA 92024 (2 copies)

Prof. Jon F. Claerbout
Department of Geophysics
Stanford University
Stanford, CA 94305

Prof. Robert W. Clayton
Seismological Laboratory
Division of Geological & Planetary Sciences
California Institute of Technology
Pasadena, CA 91125

Prof. F. A. Dahlen
Geological and Geophysical Sciences
Princeton University
Princeton, NJ 08544-0636

Prof. Adam Dziewonski
Hoffman Laboratory
Harvard University
20 Oxford St
Cambridge, MA 02138

Prof. John Ebel
Department of Geology & Geophysics
Boston College
Chestnut Hill, MA 02167

Eric Fielding
SNEE Hall
INSTOC
Cornell University
Ithaca, NY 14853

Prof. Donald Forsyth
Department of Geological Sciences
Brown University
Providence, RI 02912

Dr. Cliff Frolich
Institute of Geophysics
8701 North Mopac
Austin, TX 78759

Dr. Anthony Gangi
Texas A&M University
Department of Geophysics
College Station, TX 77843

Dr. Freeman Gilbert
Inst. of Geophysics & Planetary Physics
University of California, San Diego
P.O. Box 109
La Jolla, CA [illegible]

Mr. Edward Giller
Pacific Sierra Research Corp.
1401 Wilson Boulevard
Arlington, VA 22209

Dr. Jeffrey W. Given
SAIC
10260 Campus Point Drive
San Diego, CA 92121

Prof. Roy Greenfield
Geosciences Department
403 Deike Building
The Pennsylvania State University
University Park, PA 16802

Dan N. Hagedorn
Battelle
Pacific Northwest Laboratories
Battelle Boulevard
Richland, WA 99352

Kevin Hutchenson
Department of Earth Sciences
St. Louis University
3507 Laclede
St. Louis, MO 63103

Prof. Thomas H. Jordan
Department of Earth, Atmospheric
and Planetary Sciences
Massachusetts Institute of Technology
Cambridge, MA 02139

Robert C. Kemerait
ENSCO, Inc.
445 Pineda Court
Melbourne, FL 32940

William Kikendall
Teledyne Geotech
3401 Shiloh Road
Garland, TX 75041

Prof. Leon Knopoff
University of California
Institute of Geophysics & Planetary Physics
Los Angeles, CA 90024

Prof. L. Timothy Long
School of Geophysical Sciences
Georgia Institute of Technology
Atlanta, GA 30332

Prof. Art McGarr
Mail Stop 977
Geological Survey
345 Middlefield Rd.
Menlo Park, CA 94025

Dr. George Mellman
Sierra Geophysics
11255 Kirkland Way
Kirkland, WA 98033

Prof. John Nabelek
College of Oceanography
Oregon State University
Corvallis, OR 97331

Prof. Geza Nagy
University of California, San Diego
Department of Ames, M.S. B-010
La Jolla, CA 92093

Prof. Amos Nur
Department of Geophysics
Stanford University
Stanford, CA 94305

Prof. Jack Oliver
Department of Geology
Cornell University
Ithaca, NY 14850

Prof. Robert Phinney
Geological & Geophysical Sciences
Princeton University
Princeton, NJ 08544-0636

Dr. Paul Pomeroy
Rondout Associates
P.O. Box 224
Stone Ridge, NY 12484

Dr. Jay Pulli
RADIX System, Inc.
2 Taft Court, Suite 203
Rockville, MD 20850

Dr. Norton Rimer
S-CUBED
A Division of Maxwell Laboratory
P.O. Box 1620
La Jolla, CA 92038-1620

Prof. Larry J. Ruff
Department of Geological Sciences
1006 C.C. Little Building
University of Michigan
Ann Arbor, MI 48109-1063

Dr. Richard Sailor
TASC Inc.
55 Walkers Brook Drive
Reading, MA 01867

John Sherwin
Teledyne Geotech
3401 Shiloh Road
Garland, TX 75041

Prof. Robert Smith
Department of Geophysics
University of Utah
1400 East 2nd South
Salt Lake City, UT 84112

Prof. S. W. Smith
Geophysics Program
University of Washington
Seattle, WA 98195

Dr. Stewart W. Smith
Geophysics AK-50
University of Washington
Seattle, WA 98195

Dr. George Sutton
Rondout Associates
P.O. Box 224
Stone Ridge, NY 12484

Prof. L. Sykes
Lamont-Doherty Geological Observatory
of Columbia University
Palisades, NY 10964

Prof. Pradeep Talwani
Department of Geological Sciences
University of South Carolina
Columbia, SC 29208

Prof. Ta-liang Teng
Center for Earth Sciences
University of Southern California
University Park
Los Angeles, CA 90089-0741

Dr. R.B. Tittmann
Rockwell International Science Center
1049 Camino Dos Rios
P.O. Box 1085
Thousand Oaks, CA 91360

Dr. Gregory van der Vink
IRIS, Inc.
1616 North Fort Myer Drive
Suite 1440
Arlington, VA 22209

Professor Daniel Walker
University of Hawaii
Institute of Geophysics
Honolulu, HI 96822

William R. Walter
Seismological Laboratory
University of Nevada
Reno, NV 89557

Dr. Gregory Wojcik
Weidlinger Associates
4410 El Camino Real
Suite 110
Los Altos, CA 94022

Prof. John H. Woodhouse
Hoffman Laboratory
Harvard University
20 Oxford St.
Cambridge, MA 02138

Prof. Francis T. Wu
Department of Geological Sciences
State University of New York
at Binghamton
Vestal, NY 13901

Dr. Gregory B. Young
ENSCO, Inc.
5400 Port Royal Road
Springfield, VA 22151-2388

Dr. Ralph Alewine III
DARPA/NMRO
1400 Wilson Boulevard
Arlington, VA 22209-2308

Mr. James C. Battis
GL/LWH
Hanscom AFB, MA 01731-5000

Dr. Robert Blandford
DARPA/NMRO
1400 Wilson Boulevard
Arlington, VA 22209-2308

Eric Chael
Division 9241
Sandia Laboratory
Albuquerque, NM 87185

Dr. John J. Cipar
GL/LWH
Hanscom AFB, MA 01731-5000

Mr. Jeff Duncan
Office of Congressman Markey
2133 Rayburn House Bldg.
Washington, DC 20515

Dr. Jack Evernden
USGS - Earthquake Studies
345 Middlefield Road
Menlo Park, CA 94025

Art Frankel
USGS
922 National Center
Reston, VA 22092

Dr. T. Hanks
USGS
Nat'l Earthquake Research Center
345 Middlefield Road
Menlo Park, CA 94025

Dr. James Hannon
Lawrence Livermore Nat'l Laboratory
P.O. Box 808
Livermore, CA 94550

Paul Johnson
ESS-4, Mail Stop J979
Los Alamos National Laboratory
Los Alamos, NM 87545

Janet Johnston
GL/LWH
Hanscom AFB, MA 01731-5000

Dr. Katharine Kadinsky-Cade
GL/LWH
Hanscom AFB, MA 01731-5000

Ms. Ann Kerr
IGPP, A-025
Scripps Institute of Oceanography
University of California, San Diego
La Jolla, CA 92093

Dr. Max Koontz
US Dept of Energy/DP 5
Forrestal Building
1000 Independence Avenue
Washington, DC 20585

Dr. W.H.K. Lee
Office of Earthquakes, Volcanoes,
& Engineering
345 Middlefield Road
Menlo Park, CA 94025

Dr. William Leith
U.S. Geological Survey
Mail Stop 928
Reston, VA 22092

Dr. Richard Lewis
Director, Earthquake Engineering & Geophysics
U.S. Army Corps of Engineers
Box 631
Vicksburg, MS 39180

James F. Lewkowicz
GL/LWH
Hanscom AFB, MA 01731-5000

Mr. Alfred Lieberman
ACDA/VI-OA'State Department Bldg
Room 5726
320 - 21st Street, NW
Washington, DC 20451

Stephen Mangino
GL/LWH
Hanscom AFB, MA 01731-5000

Dr. Robert Masse
Box 25046, Mail Stop 967
Denver Federal Center
Denver, CO 80225

Art McGarr
U.S. Geological Survey, MS-977
345 Middlefield Road
Menlo Park, CA 94025

Richard Morrow
ACDA/VI, Room 5741
320 21st Street N.W
Washington, DC 20451

Dr. Keith K. Nakanishi
Lawrence Livermore National Laboratory
P.O. Box 808, L-205
Livermore, CA 94550

Dr. Carl Newton
Los Alamos National Laboratory
P.O. Box 1663
Mail Stop C335, Group ESS-3
Los Alamos, NM 87545

Dr. Kenneth H. Olsen
Los Alamos Scientific Laboratory
P.O. Box 1663
Mail Stop C335, Group ESS-3
Los Alamos, NM 87545

Howard J. Patton
Lawrence Livermore National Laboratory
P.O. Box 808, L-205
Livermore, CA 94550

Mr. Chris Paine
Office of Senator Kennedy
SR 315
United States Senate
Washington, DC 20510

Colonel Jerry J. Perrizo
AFOSR/NP, Building 410
Bolling AFB
Washington, DC 20332-6448

Dr. Frank F. Pilotte
HQ AFTAC/TT
Patrick AFB, FL 32925-6001

Katie Poley
CIA-OSWR/NED
Washington, DC 20505

Mr. Jack Rachlin
U.S. Geological Survey
Geology, Rm 3 C136
Mail Stop 928 National Center
Reston, VA 22092

Dr. Robert Reinke
WL/NTESG
Kirtland AFB, NM 87117-6008

Dr. Byron Ristvet
HQ DNA, Nevada Operations Office
Attn: NVCG
P.O. Box 98539
Las Vegas, NV 89193

Dr. George Rothe
HQ AFTAC/TTR
Patrick AFB, FL 32925-6001

Dr. Alan S. Ryall, Jr.
DARPA/NMRO
1400 Wilson Boulevard
Arlington, VA 22209-2308

Dr. Michael Shore
Defense Nuclear Agency/SPSS
6801 Telegraph Road
Alexandria, VA 22310

Dr. Albert Smith
Los Alamos National Laboratory
L-205
P. O. Box 808
Livermore, CA 94550

Donald L. Springer
Lawrence Livermore National Laboratory
L-205
P. O. Box 808
Livermore , CA 94550

Mr. Charles L. Taylor
GL/LWG
Hanscom AFB, MA 01731-5000

Mr. Steven R. Taylor
Lawrence Livermore National Laboratory
L-205
P. O. Box 808
Livermore, CA 94550

Dr. Eileen Vergino
Lawrence Livermore National Laboratory
L-205
P. O. Box 808
Livermore, CA 94550

Dr. Thomas Weaver
Los Alamos National Laboratory
P.O. Box 1663, Mail Stop C335
Los Alamos, NM 87545

J.J. Zucca
Lawrence Livermore National Laboratory
P. O. Box 808
Livermore, CA 94550

GL/SULL
Research Library
Hanscom AFB , MA 01731-5000 (2 copies)

Secretary of the Air Force
(SAFRD)
Washington, DC 20330

Office of the Secretary Defense
DDR & E
Washington, DC 20330

HQ DNA
Attn: Technical Library
Washington, DC 20305

DARPA/RMO/RETRIEVAL
1400 Wilson Boulevard
Arlington, VA 22209

DARPA/RMO/Security Office
1400 Wilson Boulevard
Arlington, VA 22209

Geophysics Laboratory
Attn: XO
Hanscom AFB, MA 01731-5000

Geophysics Laboratory
Attn: LW
Hanscom AFB, MA 01731-5000

DARPA/PM
1400 Wilson Boulevard
Arlington, VA 22209

Defense Technical Information Center
Cameron Station
Alexandria, VA 22314 (2 copies)

Defense Intelligence Agency
Directorate for Scientific
& Technical IntelligenceAttn: DT1B
Washington, DC 20340-6158

AFTAC/CA
(STINFO)
Patrick AFB, FL 32925-6001

TACTEC
Battelle Memorial Institute
505 King Avenue
Columbus, OH 43201 (Final Report Only)

Dr. Ramon Cabre, S.J.
Observatorio San Calixto
Casilla 5939
La Paz, Bolivia

Prof. Hans-Peter Harjes
Institute for Geophysik
Ruhr University/Bochum
P.O. Box 102148
4630 Bochum 1, FRG

Prof. Eystein Husebye
NTNF/NORSAR
P.O. Box 51
N-2007 Kjeller, NORWAY

Prof. Brian L.N. Kennett
Research School of Earth Sciences
Institute of Advanced Studies
G.P.O. Box 4
Canberra 2601, AUSTRALIA

Dr. Bernard Massinon
Societe Radiomana
27 rue Claude Bernard
75005 Paris, FRANCE (2 Copies)

Dr. Pierre Mecheler
Societe Radiomana
27 rue Claude Bernard
75005 Paris, FRANCE

Dr. Svein Mykkeltveit
NTNF/NORSAR
P.O. Box 51
N-2007 Kjeller, NORWAY

FOREIGN (Others)

Dr. Peter Basham
Earth Physics Branch
Geological Survey of Canada
1 Observatory Crescent
Ottawa, Ontario, CANADA K1A 0Y3

Dr. Eduard Berg
Institute of Geophysics
University of Hawaii
Honolulu, HI 96822

Dr. Michel Bouchon
I.R.I.G.M.-B.P. 68
38402 St. Martin D'Heres
Cedex, FRANCE

Dr. Hilmar Bungum
NTNF/NORSAR
P.O. Box 51
N-2007 Kjeller, NORWAY

Dr. Michel Campillo
Observatoire de Grenoble
I.R.I.G.M.-B.P. 53
38041 Grenoble, FRANCE

Dr. Kin Yip Chun
Geophysics Division
Physics Department
University of Toronto
Ontario, CANADA M5S 1A7

Dr. Alan Douglas
Ministry of Defense
Blacknest, Brimpton
Reading RG7-4RS, UNITED KINGDOM

Dr. Roger Hansen
NTNF/NORSAR
P.O. Box 51
N-2007 Kjeller, NORWAY

Dr. Manfred Henger
Federal Institute for Geosciences & Nat'l Res.
Postfach 510153
D-3000 Hanover 51, FRG

Ms. Eva Johannisson
Senior Research Officer
National Defense Research Inst.
P.O. Box 27322
S-102 54 Stockholm, SWEDEN

Dr. Fekadu Kebede
Seismological Section
Box 12019
S-750 Uppsala, SWEDEN

Dr. Tormod Kvaerna
NTNF/NORSAR
P.O. Box 51
N-2007 Kjeller, NORWAY

Dr. Peter Marshal
Procurement Executive
Ministry of Defense
Blacknest, Brimpton
Reading FG7-4RS, UNITED KINGDOM

Prof. Ari Ben-Menahem
Department of Applied Mathematics
Weizman Institute of Science
Rehovot, ISRAEL 951729

Dr. Robert North
Geophysics Division
Geological Survey of Canada
1 Observatory Crescent
Ottawa, Ontario, CANADA K1A 0Y3

Dr. Frode Ringdal
NTNF/NORSAR
P.O. Box 51
N-2007 Kjeller, NORWAY

Dr. Jorg Schlittenhardt
Federal Institute for Geosciences & Nat'l Res.
Postfach 510153
D-3000 Hannover 51, FEDERAL REPUBLIC OF GERMANY